Institut für Chemie 3:
Atmosphärische Chemie

Sources and distribution of NO_x in the upper troposphere at northern midlatitudes

D.H. Ehhalt
F. Rohrer
A. Wahner

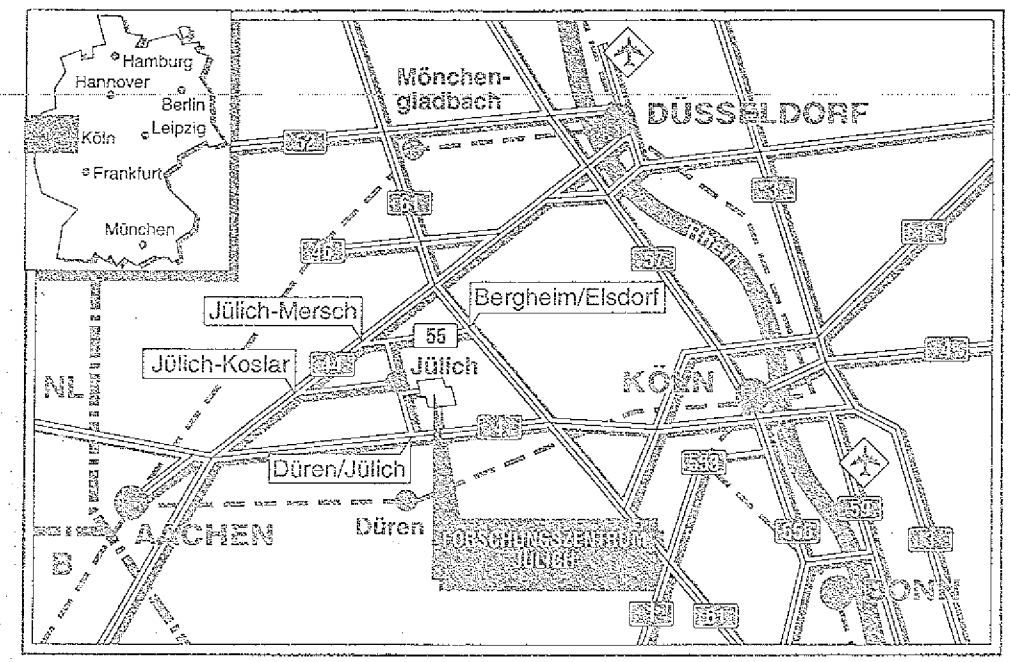

Berichte des Forschungszentrums Jülich ; 2488
ISSN 0366-0885
Institut für Chemie 3: Atmosphärische Chemie Jül-2488

Zu beziehen durch: Forschungszentrum Jülich GmbH · Zentralbibliothek
Postfach 1913 · D-5170 Jülich · Bundesrepublik Deutschland
Telefon: 02461/61-6102 · Telefax: 02461/61-6103 · Telex: 833556-70 kfa d

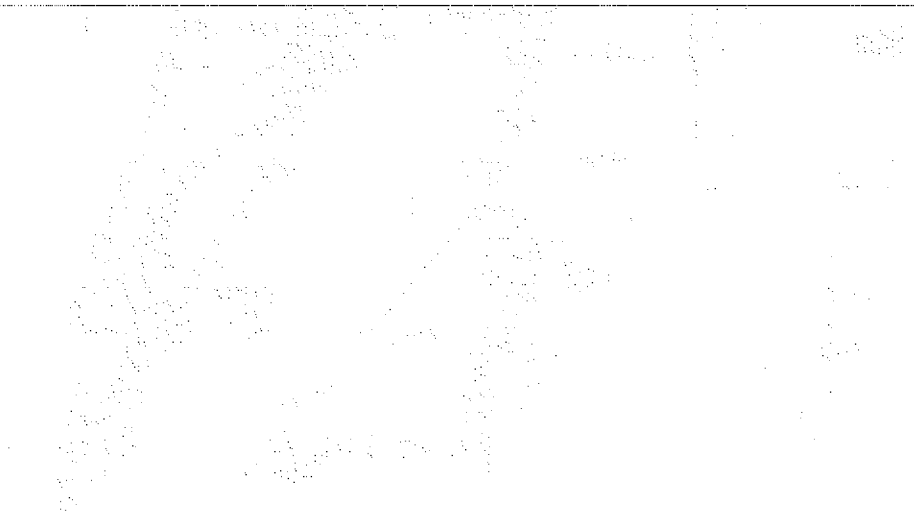

Sources and distribution of NO_x in the upper troposphere at northern midlatitudes

D.H. Ehhalt
F. Rohrer
A. Wahner

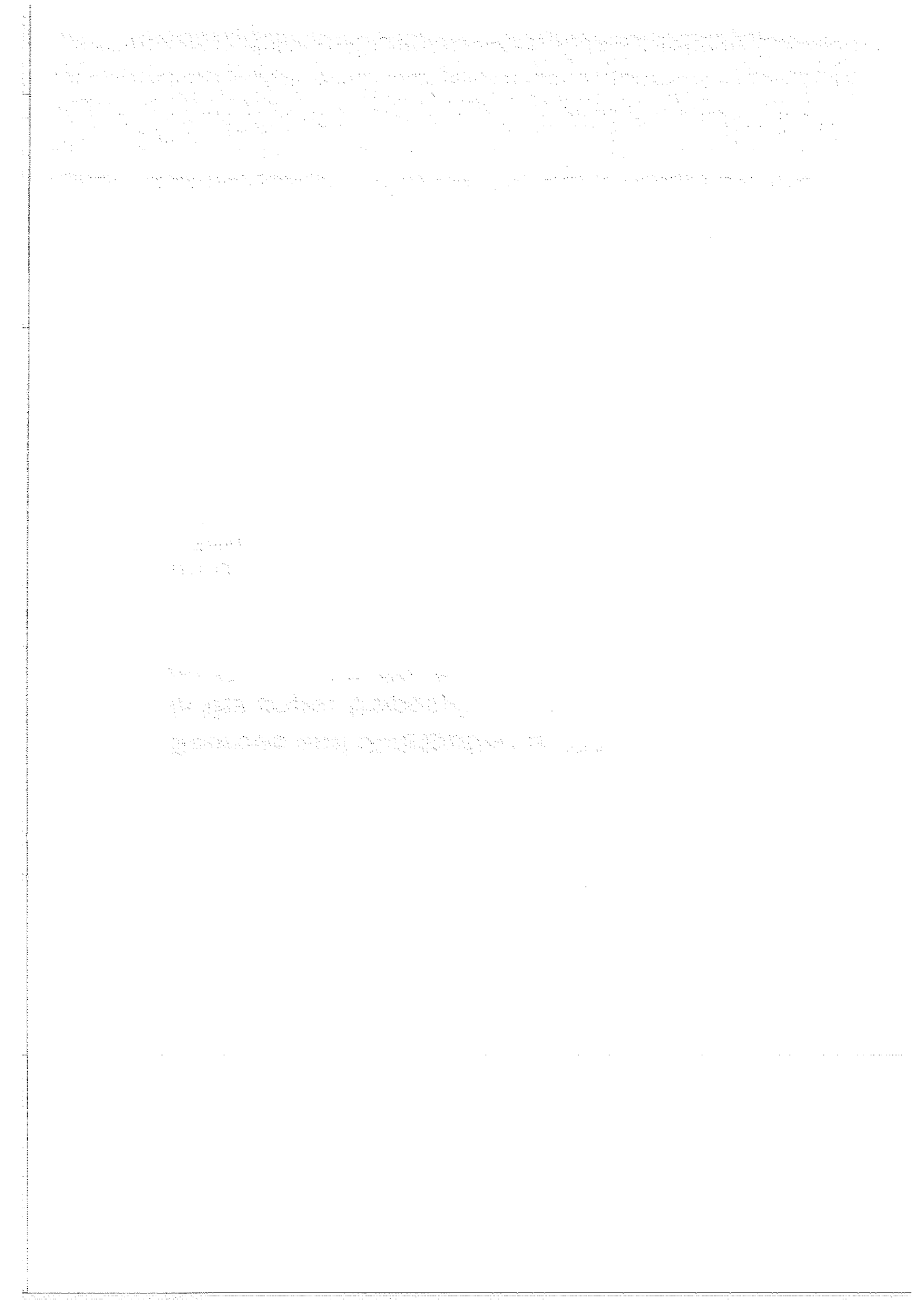

Table of Contents

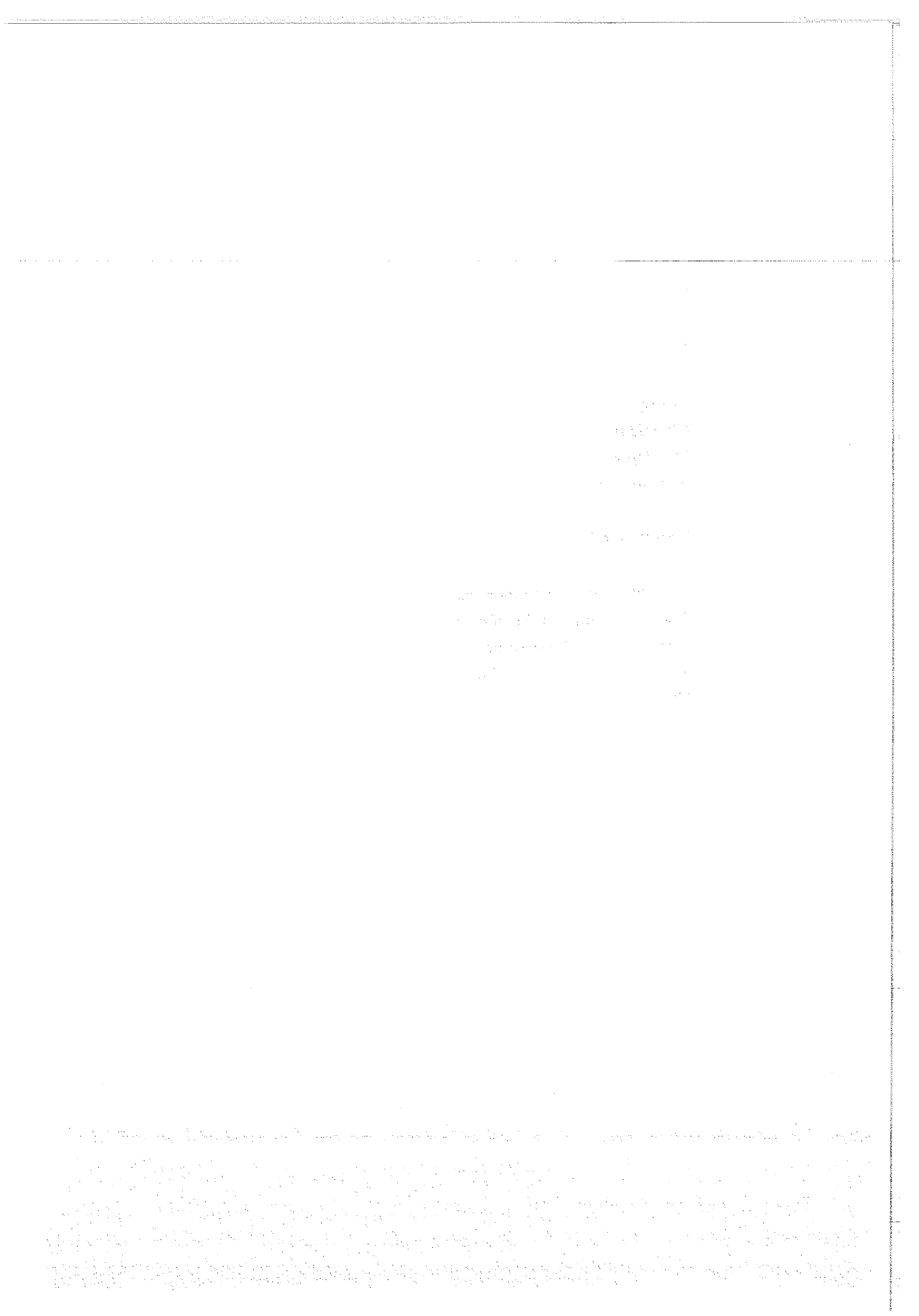

Sources and distribution of NO_x in the upper troposphere at northern midlatitudes

D.H. Ehhalt, F. Rohrer, and A. Wahner

Institut für Atmosphärische Chemie

Forschungszentrum Jülich

Postfach 1913, D-5170 Jülich

ABSTRACT

A simple quasi 2-D model is used to study the zonal distribution of NO_x. The model includes vertical transport in form of eddy diffusion and deep convection, zonal transport by a vertically uniform wind, and a simplified chemistry of NO, NO_2 and HNO_3. The NO_x sources considered are surface emissions (mostly from the combustion of fossil fuel), lightning, aircraft emissions, and downward transport from the stratosphere. The model is applied to the latitude band of 40°N to 50°N during the month of June; the contributions to the zonal NO_x distribution from the individual sources and transport processes are investigated. The model predicted NO_x concentration in the upper troposphere is dominated by air lofted from the polluted planetary boundary layer over the large industrial areas of Eastern North America and Europe. Aircraft emissions are also important and contribute on average 30 %. Stratospheric input is minor about 10 %, less even than that by lightning. The model provides a clear indication of intercontinental transport of NO_x and HNO_3 in the upper troposphere. Comparison of the modelled NO profiles over the Western Atlantic with those measured during STRATOZ III in 1984 shows good agreement at all altitudes.

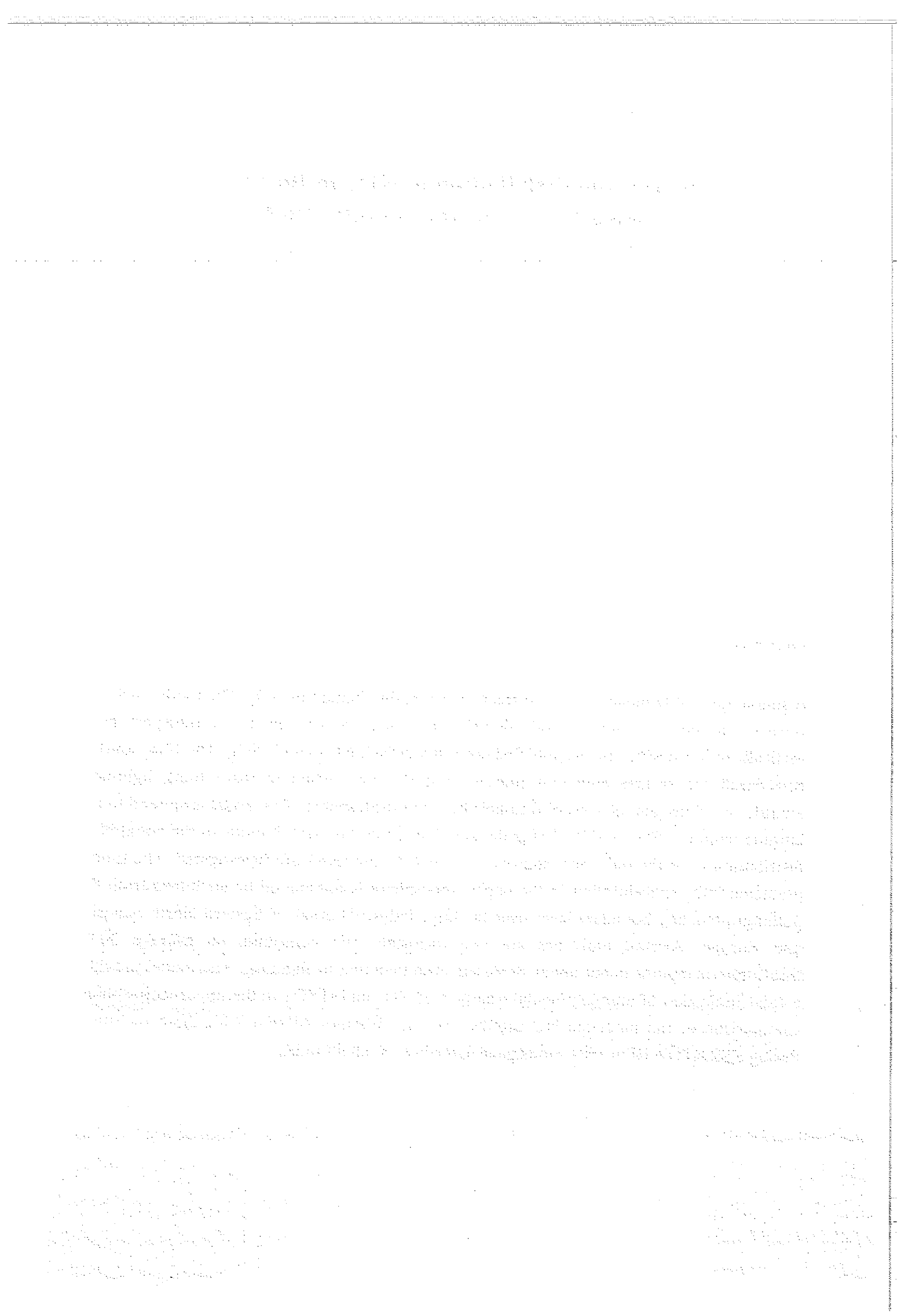

1. INTRODUCTION

The nitrogen oxides, NO and NO_2, play a dual role in tropospheric chemistry: They are a major controlling factor in the concentration of the hydroxyl radical, OH. Even more important, they are primarily responsible for the tropospheric formation of ozone, O_3, and it is the anthropogenic emission of NO in various combustion processes that causes the increase in tropospheric O_3 concentration observed at northern midlatitudes. Because O_3 is a greenhouse gas anthropogenic emissions of NO can thus also have an impact on climate. Moreover, since the temperature increase at the earth's surface is predicted to be particularly sensitive to the O_3 concentrations in the upper troposphere [Wang et al., 1980], relatively small emissions of NO_x into the upper troposphere, by air traffic for instance, can play an unexpectedly large role.

Considering the importance of the nitrogen oxides, $NO_x = NO + NO_2$, relatively few measurements exist to define their global distribution. Even less is known about the distribution of NO_x in the upper troposphere and man's impact on it.

A major fraction of the available measurements of NO in the upper troposphere were published by Drummond et al. [1988]. They were made during the STRATOZ III aircraft campaign in June 1984 mainly along the coast lines of North America, South America, eastern North Africa and Europe between 70°N and 60°S latitude and from 0 km to 12 km altitude. Figure 1 presents an integrated view of these measurements. It is a different rendering of Figure 8 by Ehhalt and Drummond [1988] in which all the data were averaged into a grid of 1 km altitude by 10° latitude boxes and filtered to remove excursions and gaps. The measurements in the boundary layer were excluded to prevent propagation of the high boundary values into the atmospheric layer between 1 km and 2 km altitude. The most conspicuous feature in this 2-dimensional representation is the large hump of high NO concentrations in the upper troposphere extending all over the northern hemisphere and down to about 30°S latitude. A closer inspection shows the highest NO concentrations to occur occasionally below the highest altitudes, generating NO maxima at 10 - 11 km altitude. This is even more obvious in the individual vertical profiles [Drummond et al., 1988]. This, together with other patterns in the observed NO distribution, namely low NO concentrations in the upper troposphere over the oceans or south of 30°S, made it clear from the beginning that stratospheric input could not have been the sole source of the high NO concentrations observed in the upper troposphere during STRATOZ III.

Thus Drummond et al. [1988] also considered other sources, namely emissions by high flying aircraft, NO_x produced by lightning, and fast vertical transport from the planetary boundary layer over the continents. The last process, which had already been suggested by Gidel [1983] and observed using short lived non methane hydrocarbons, NMHC, by Ehhalt et al. [1985]. seemed particularly promising, because during STRATOZ III also high concentrations of short-lived NMHC were observed in the upper troposphere [Rudolph, 1988] indicating the

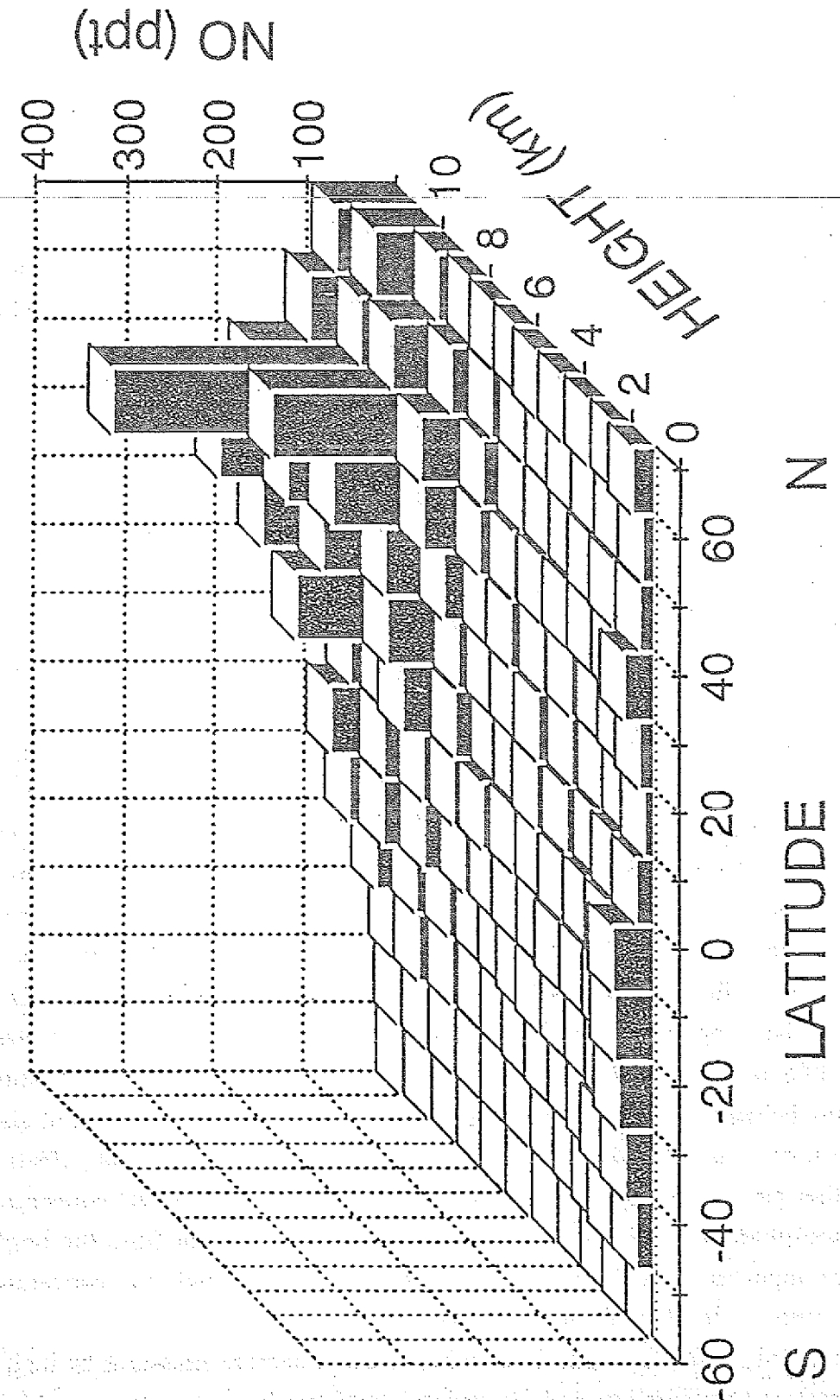

Figure 1 Meridonal representation of the average NO mixing ratios measured during STRATOZ III along the coast lines of Eastern North America, South America, North Western Africa and Europe.

action of fast vertical transport. In fact the vertical concentration profile of ethene averaged over 30°N - 70°N latitude showed a clear maximum between 10 and 11 km altitude [Ehhalt, 1988].
Unfortunately, the observed patterns in the NO distribution were by themselves not sufficient to provide a quantitative estimate of the contributions from the various sources [Drummond et al., 1988]. The hope of using correlations with the concentration of other trace gases measured during STRATOZ III, above all O_3 and CO, to obtain such an estimate also proved vain so far. So in this paper we attempt to use a model to quantify the impact of the various sources mentioned.
This will be the most simple model with which we can hope to describe the salient features of the vertical distribution of NO in the troposphere. Since we are interested in studying the role of aircraft emissions, the model will be applied to 40°-50°N latitude where these emissions are relatively large, and it will be applied to the month of June, because then all the mentioned source processes are active and we will be able to compare the model profiles against the STRATOZ III data. Finally we will compare the model results to other published experimental and model data on the tropospheric NO_x cycle.

2. MODEL DESCRIPTION

What are the minimum requirements a model must have, to reproduce the salient features in the observed vertical NO profiles ? Firstly, after what has been said above, it needs to include a mechanism for fast vertical transport. Secondly, it needs some form of horizontal transport: The surface sources of NO show large horizontal gradients especially near the coast lines, where the oceans show virtually no, and the densely populated continental plains quite large NO emissions. As a consequence, air carried upward by fast vertical transport over the strong source areas will inject plumes of high NO_x concentrations into inland moving clean oceanic air and thus modify the shape of the vertical NO profiles with increasing distance down wind. Thus we have to expect the vertical profile of NO to change in the horizontal direction depending on the airmass trajectory.
Thirdly, the model has to include a chemistry which considers the fast interchange of NO with NO_2 and conversion of NO_x to a compound which is soluble and can be rained out, e.g. HNO_3.
Finally the model needs to incorporate the salient features of the source distributions.

Transport

To remain simple the transport is simulated by a time dependent 1-dimensional model which treats only the vertical transport explicitly. It covers the altitudes from 0-14 km with a 1 km height resolution except for the two lowest levels which are located at 0.1 and 0.5 km. The tropopause is located at 12 km altitude. Temperature and density profiles are those of the US Standard Atmosphere [1976]. The mechanism for the fast vertical transport is shown schematically in Figure 2. It is a random process and superimposed onto a continuous transport by eddy diffusion whose profile is shown in Figure 3. At each time step a random number is selected which specifies whether a fast transport event takes place and into which height level air from the boundary layer is to be lofted. A fixed fraction of air at the receiving level, 1 %, is then replaced by air from the 1 km level. To maintain mass balance, the corresponding density weighted amounts of air are shifted downward from each of the lower levels to the next. The frequency of the transport events is chosen to match the exchange rate profiles shown in Figure 3. They are different above ocean and land and apply to the summer months at 44°N to 52°N latitude. They were taken from the convection statistics of the General Circulation Model developed at the Goddard Institute of Space Studies (M. Prather, private communication). The most important feature for the present purpose is the maximum in the profile of the continental exchange rate between 8 and 10 km altitudes, which indicates that air in those altitudes is replaced every 10 days by boundary layer air.

The stochastic treatment of the fast vertical transport is not required for the problem at hand. It could just as well be replaced by a continuous injection corresponding to the exchange rate profile given in Figure 3. It was kept for convenience, since it had been installed in some previous runs in which we tried to study the variance in the vertical NO profiles.

The horizontal transport component in the model is introduced by allowing the NO_x source terms, boundary conditions, and vertical transport to change in time commensurate with a horizontal displacement by a 8 ms^{-1} westerly wind at 40°-50°N latitude. This is equivalent to moving the whole air column treated in the model zonally around the globe with a vertically uniform wind speed. The wind speed corresponds to the zonally and vertically averaged west wind component in June at 40°-50°N latitude (Houghton, 1985). It takes about 40 days to circle the globe or 35000 time steps of 100 s.

Chemistry

The model allows two nitrogen compounds to be transported, namely $NO_x = NO + NO_2$ and HNO_3, whose concentrations are interlinked by the chemical reactions (1) to (10).

Reactions (1) and (2):

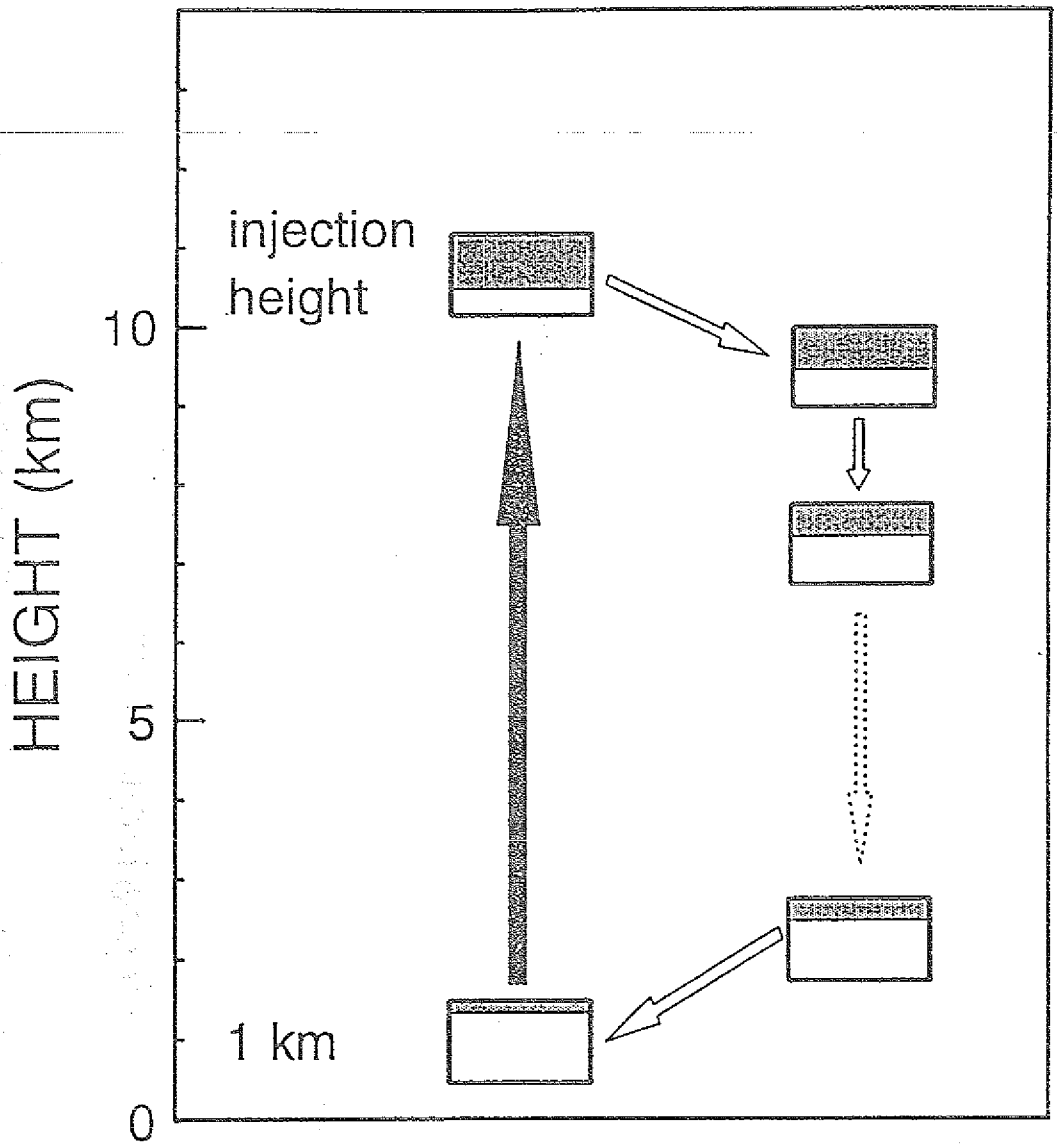

Figure 2 Schematic of the parameterisation of fast vertical transport by convection implemented in the model (see text).

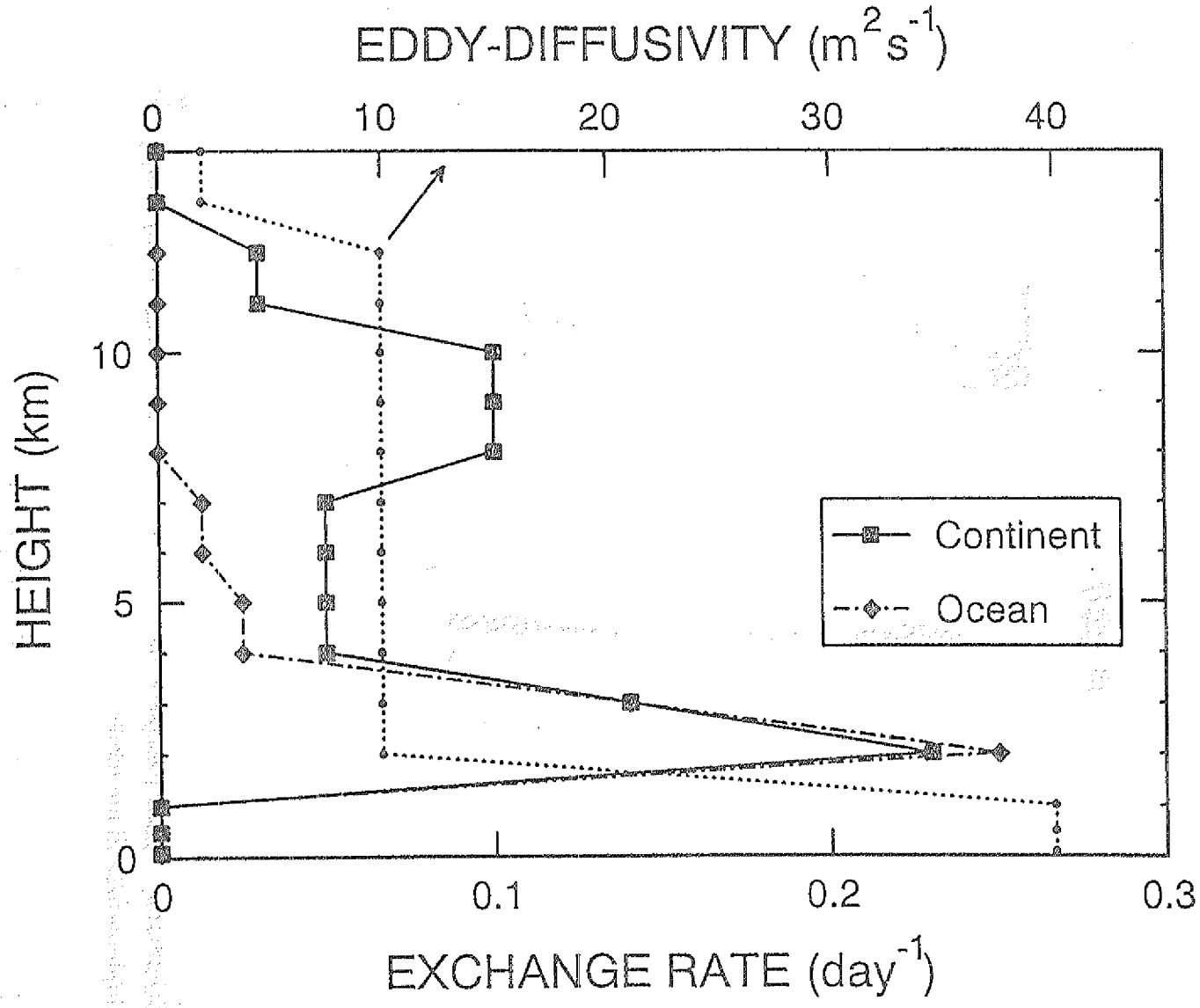

Figure 3 Vertical profiles of the exchange rates of the fast vertical transport over the ocean (dashed-dotted line) and over the continent (solid line). The vertical profile of Eddy-diffusivity is given by the dotted line (top scale).

$$NO + O_3 \rightarrow NO_2 + O_2 \quad (1)$$
$$NO_2 + h\nu \rightarrow NO + O \quad (2)$$

establish a fast photochemical equilibrium between NO and NO_2 which is reached within a matter of minutes - the main reason for lumping the nitrogen oxides into NO_x.
Where needed, the fraction of NO_x present as NO or NO_2 is computed from those reactions assuming photochemical equilibrium:

$$[NO]/[NO_x] = J_2/(J_2 + k_1[O_3]) \quad (3)$$
$$[NO_2]/[NO_x] = k_1[O_3]/(J_2 + k_1[O_3]) \quad (4)$$

where k_1 is the rate constant for reaction (1) and J_2 the photolysis rate for reaction (2). NO_2 is eventualy converted to HNO_3 through the addition reaction with the hydroxyl radical, OH.

$$NO_2 + OH \xrightarrow{M} HNO_3 \quad (5)$$

The resulting nitric acid molecules are allowed to convert back to NO_2 via the reactions

$$HNO_3 + h\nu \rightarrow NO_2 + OH \quad (6)$$
$$HNO_3 + OH \rightarrow NO_2 + H_2O \quad (7)$$

However, these back reactions have relatively slow rates and are not very important for the model results.

The model also allows for some night time chemistry through the reactions

$$NO_2 + O_3 \rightarrow NO_3 + O_2 \quad (8)$$

and conversion of NO_3 to HNO_3 via a net reaction of the type

$$NO_3 \xrightarrow{H_2O_{fl}} HNO_3 \quad (9)$$

During the sunlit periods NO_3 is photolysed

$$NO_3 + h\nu \rightarrow NO + O_2 \quad (10)$$

During the summer conditions treated here the day time conversion of NO_2 to HNO_3 through reaction (5) with OH is by far the most important. The night time reaction (8) via NO_3 contributes less than 20 % to the loss of NO_x.

The vertical concentration profiles of OH and O_3, as well as the profiles of the photolysis rates for NO_2 and HNO_3, which are needed to promote reactions (1) to (10), are held fixed at their diurnally (24h) averaged values. They were taken from a 1-D model calculation with fully treated chemistry and solar UV radiation for 45°N and June (Röth, 1986). The averaged NO_3 photolysis rate was properly weighted to take account of the fact that during nighttime NO_x is present as NO_2 only. The OH and O_3 concentration profiles are shown in Figure 4. They agree well with the OH profile at 45°N by Volz et al [1981], and the average O_3 profile measured during STRATOZ III at 45°N, respectively [Marenco and Said, 1989]. The rate constants used are those given in JPL [1990]. The resulting profiles of the total chemical lifetimes for NO_x and HNO_3 are shown in Figure 5. The long life time of NO_x in the upper troposphere is partly due to the low $[NO_2]/[NO]$ ratio at these altitudes. The vertical profile of the $[NO]/[NO_x]$ ratio is also shown in Figure 5.

Dry deposition and rainout

The nitrogen compounds are eventually removed from the atmosphere by dry deposition at the earth's surface and washout by precipitation. The model allows HNO_3 to dry deposit on all surfaces with a deposition velocity of 2 cm s^{-1} [cf. Huebert and Robert, 1985], a value which for a global average may be a bit on the high side considering the lumped nature of HNO_3 in this model (see below). NO_2 is deposited on land surfaces only with a deposition velocity of 0.5 cm s^{-1}; its deposition on the ocean surface is negligibly small [Boettger et al., 1978]. NO is not dry deposited.

Washout removes only HNO_3, the one higly water soluble species in the model.
It occurs in two modes: One which might be considered in-cloud scavenging, another which might be considered entrainment and below-cloud scavenging. The former is associated with the fast transport events which are thought to proceed through convective clouds. It can be specified by a parameter which determines what fraction of the HNO_3 lofted by such an event from the 1 km level reaches the injection altitude. In the calculations shown below the value of this parameter was set to 0.5, i.e. one half of the HNO_3 moved upward by a fast transport event is scavenged and rained out, the other half is transported to the receiving altitude. There is little guidance in the literature for the choice of this value. Our choice was guided by the consideration that our model lumps all nitrates in the term HNO_3, where some of the nitrates like peroxyacetylnitrate are little soluble, and others like aerosol nitrate are carried upward in cloud droplets and reinjected into the free air when these evaporate. Since in-cloud

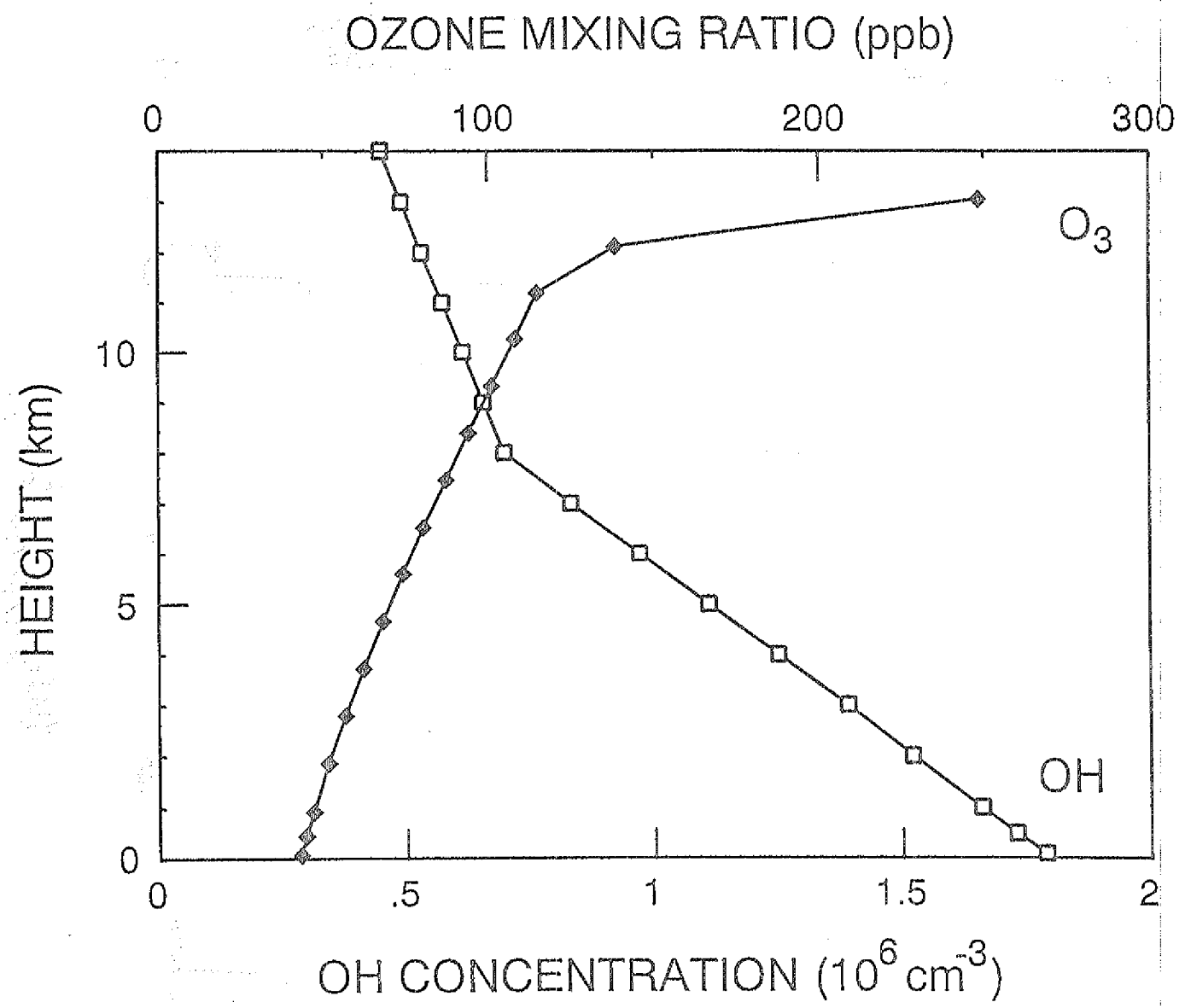

Figure 4 Vertical profiles of the OH-concentration (open squares, bottom scale) and ozone mixing ratio (closed diamonds, top scale).

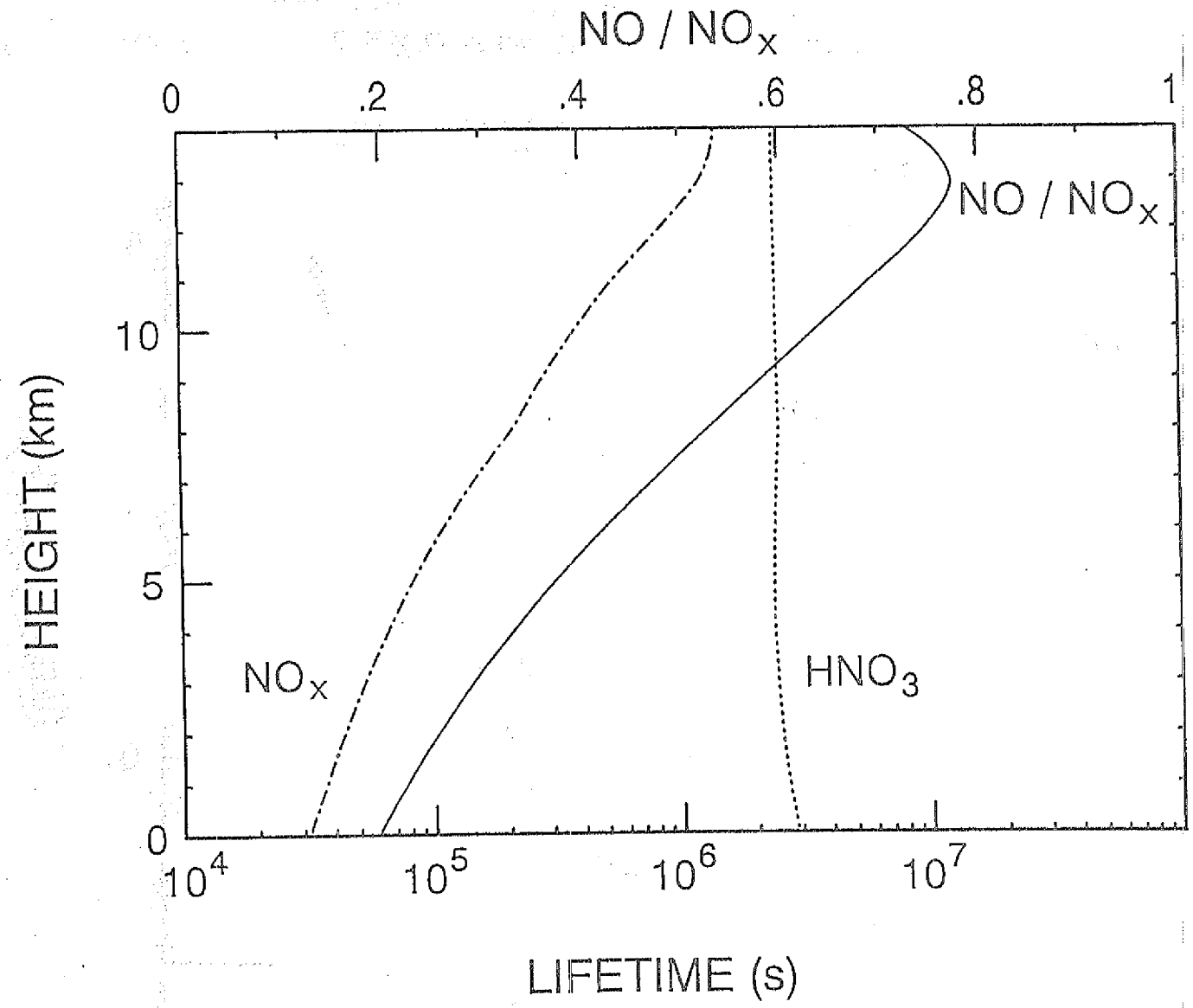

Figure 5: Vertical profiles of the total chemical lifetime of NO_x (dashed-dotted line) and HNO_3 (dotted line, bottom scale). Also shown is the calculated vertical profile of the [NO] / [NO_x] ratio (solid lines, top scale).

scavenging is of minor importance (see Table 2 below), the model results are not sensitive to this parameter.
Entrainment was treated by a removal time constant for HNO_3 of 10 days at all tropospheric altitudes above 1 km. Below-cloud scavenging was treated by reducing that time constant to 2 days at the altitudes of 1 km and below. Entrainment in the stratosphere was assumed to be zero.

NO_x sources

NO_x is released into the atmosphere, primarily as NO, from a variety of sources. The sources treated in the model and their respective emission rates in 40°-50°N latitude are listed in Table 1. All the surface sources, mainly burning of fossil fuel, with minor contributions from biomass burning, and soil emissions are lumped into one term. The emission rates in Table 1 were calculated from the global source strengths summarized in Ehhalt and Drummond [1988] and their relative latitudinal distributions given in Ehhalt and Drummond [1982], except the value for aircraft emissions which was updated for 1984, see below.

Table 1

NO_x-emissions in the 40 - 50°N latitude band for June 1984.
They are given in absolute terms and as fractions of the global strengths of the individual sources.

Source	Emission rate in 40°-50°N (10^6 tN/yr)	Fraction in 40°-50°N (%)
Surface sources		
a) total	8.63	23
b) fossil fuel burning	7.45	36
Lightning	0.29	6
Aircraft (civil)	0.081	23
Stratosphere	0.037*)	6

*) Only 1/4 of this stratospheric input is in the form of NO_x the major part is HNO_3.

The stratospheric input is treated as flux boundary condition at the uppermost level, 14 km altitude. The stratospheric input of NO_y varies with latitude and season in a manner which has not been determined directly but is generally assumed to be analogous to the input of nuclear bomb debris or stratospheric O_3. To estimate the flux at 40°-50°N latitude, we have adopted the latitudinal dependence of stratospheric NO_y input given by Ehhalt and Drummond [1982] which was based on the deposition pattern of radioactive bomb debris. We further assumed that the NO_y influx during June equals the annual average, an assumption which is suggested by the seasonal variation of the O_3 concentration in the upper troposphere above Hohenpeißenberg, 48°N latitude [Attmannspacher et al., 1984]. Both assumptions increase the uncertainty of the stratospheric input adopted here. At the same time they make it difficult to estimate that uncertainty; it is probably around a factor of two.
The adopted downward flux which totals 1.6×10^{12} molecules N $m^{-2} s^{-1}$ is split into two components, an NO_x flux of 1/4 and an HNO_3 flux of 3/4 of that value, to take account of the partitioning of the NO_y species within the stratosphere. The flux is zonally uniform. Integrated over the 40°-50°N latitude band the NO_y flux totals 0.038×10^6 t N/yr, the value given in Table 1. This is about 6 % of the global stratospheric NO_y input.

The surface source is also treated as a flux boundary condition; all that input is in the form of NO_x. The surface flux of NO_x shows a strong variation with longitude; we have tried to mimick its essential features while keeping its structure as simple as possible by adopting the longitudinal input profile shown in Figure 6.
It assumes that there is no NO_x input over the oceans and that the inputs by biomass burning, soil microbial activity and 10 % of the fossil fuel burning are uniformly distributed over the continents. The major fraction of the fossil fuel input is placed in 20° and 25° longitude wide boxes over eastern Northamerica and Europe and a small fraction in 5° wide boxes over western Northamerica and eastern Asia. This zonal distribution is based on a variety of publications [see Böttger et al., 1978; Logan, 1983] and agrees surprisingly well with the zonal distribution implicit in the global NO_x emission patterns given by Hameed and Dignon [1988]. Although the latter shows smoother transitions between the longitudes of high and low emissions, the total surface emissions of NO_x in the 40°-50°N latitude band are virtually identical. Obviously the present choice of a box-shaped profile of the surface emission rates emphasizes the contrast between low oceanic and high continental sources at the coasts. Given the fact that most of the surface emitted NO is from fossil fuel burning and that most of the emissions are over Northamerica and Europe where emission factors and fuel consumption are reasonably well known, we would assume that the surface sources in the 40°-50°N are known to about ± 30 %.

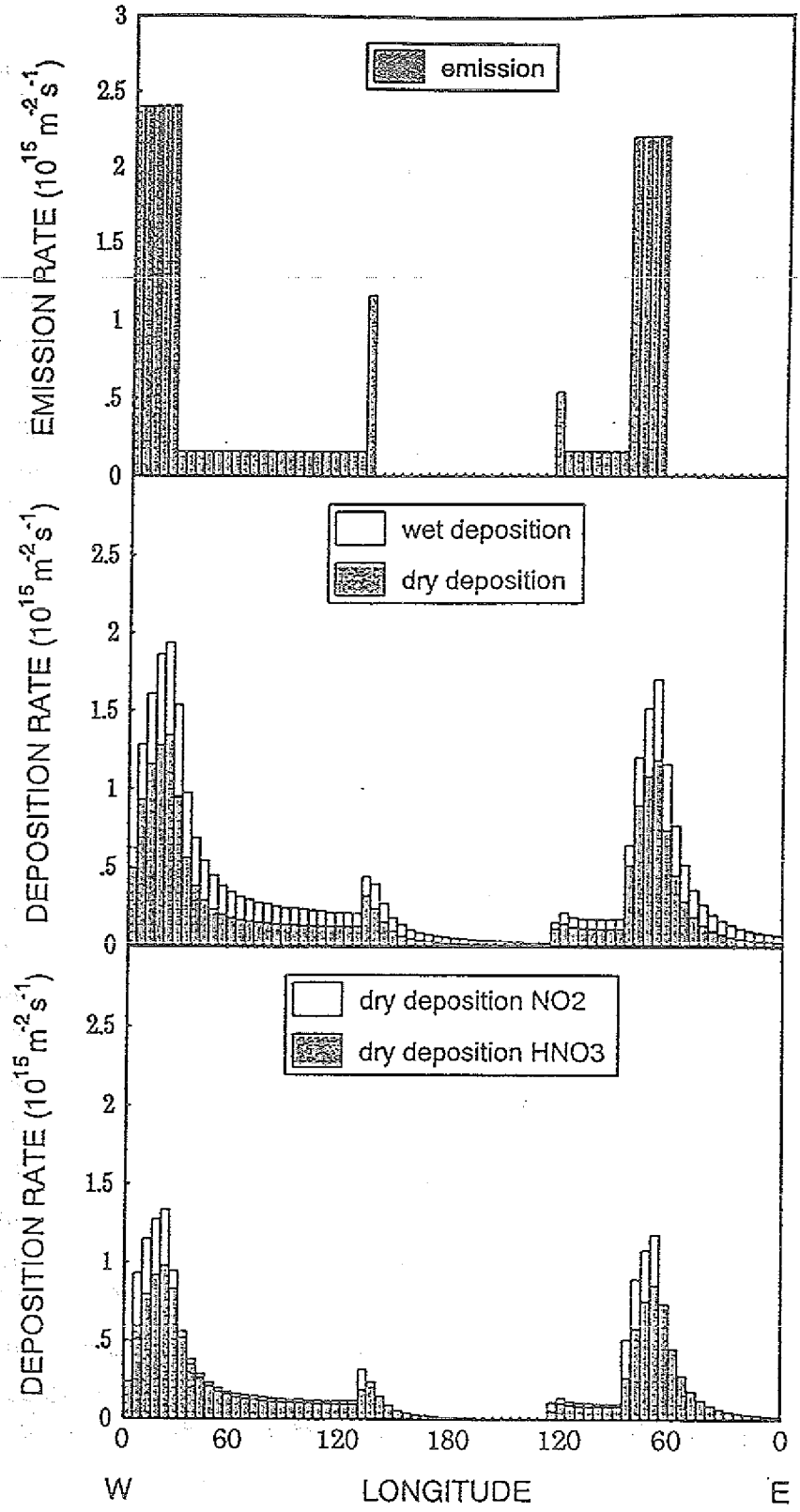

Figure 6 Longitudinal distribution of the NO_x emission and NO_y deposition rates. Top panel: Total surface emission rates for NO_x (molecules N $m^{-2}s^{-1}$) used as input for the model calculations. Middle panel: Calculated total deposition rates (molecules N $m^{-2}s^{-1}$), shaded area shows the contribution of the wet deposition, white area the contribution of the dry deposition. Bottom panel: Calculated dry deposition rates (molecules N $m^{-2}s^{-1}$), shaded area shows the contribution of NO_2 dry deposition, white area the contribution of HNO_3 dry deposition.

Lightning represents a volume source of NO_x. Its total emission rate of 0.3×10^6 t N/yr in the 40°N to 50°N latitude band was taken from Ehhalt and Drummond [1982] (see Table 1) and distributed with longitude and height according to the following considerations: Lightning is considerably less frequent over the oceans than over the continents. At 40°N to 50°N latitude the average annual number of days with thunderstorms is about 20 over the continents, 10 over the Atlantic and 5 over the Pacific (Houghton, 1985). These weight factors were also used to characterize the longitudinal distribution of the NO emission by lightning.

The vertical distribution was coupled to the fast transport by convective clouds. Since frequent and strong lightning occurs only in high thunderstorms, NO injection from lightning was only allowed for fast transport events which exceeded 8 km altitude over the continents. During such an event NO_x is introduced in equal amounts at all altitudes except for the highest altitude which receives twice that amount. Over the oceans, where in our model clouds never reach 8 km altitude, the cut off height for NO_x injection by lightning was set at 4 km. The zonally averaged height profile of the NO_x injection by lightning resulting from that procedure is shown in Figure 7.

It closely agrees with that used by Logan et al. [1981]. Because of the large uncertainty in the global estimate of the NO_x production by lightning no adjustment was made for a seasonal variation in the lightning source. Here the error in the NO_x production rate is probably larger than a factor of two.

Although the smallest contribution globally, aircraft emissions are expected to contribute significantly to the NO concentration in the upper troposphere at 40°-50°N latitude. In the present paper it is assumed that all the oxidized nitrogen compounds emitted by the aircraft is in the form of NO_x and that the average emission index is 10 g NO_2/kg fuel [Nüßer and Schmitt, 1990]. It should be noted that the value of the emission index is quite uncertain. The average fuel consumption in 1984 by the commercial aircraft was 113×10^6 t fuel/yr [Nüßer and Schmitt, 1990]. This corresponds to a global NO_x injection of 0.34×10^6 t N/yr mostly into the upper troposphere by aircraft exhaust of which 23 % are released into the 40°N to 50°N latitude. The CIAP report [1974] provides various scenarios on the future horizontal flight patterns. From it the fraction in 40° to 50°N and the longitudinal distribution of NO_x emissions in that latitude band were derived (Figure 8). Together with flight information of more modern jet aircraft [Reichow, 1990] those patterns were also used to derive the vertical distribution of NO_x emission which is also shown in Figure 7. Because of the fast increase in commercial air traffic NO_x emissions by aircraft are expected to increase too at a rate of about 7 % per year. The estimated uncertainty in the NO_x emission rate by aircraft is also a factor of two.

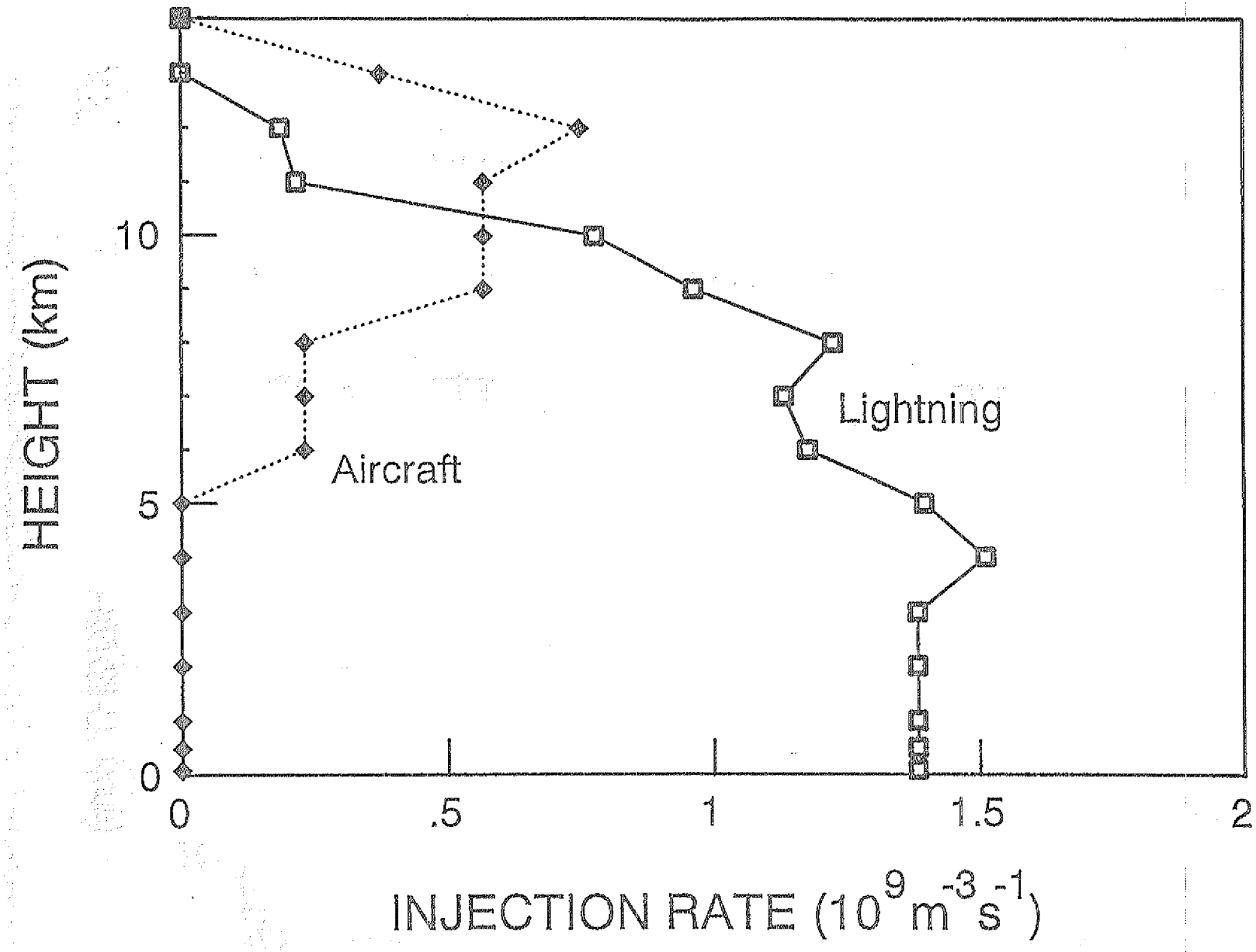

Figure 7 Vertical profile of the zonally averaged NO_x injection rate by lightning (open squares) and aircraft (closed diamonds) used as input for the model calculations.

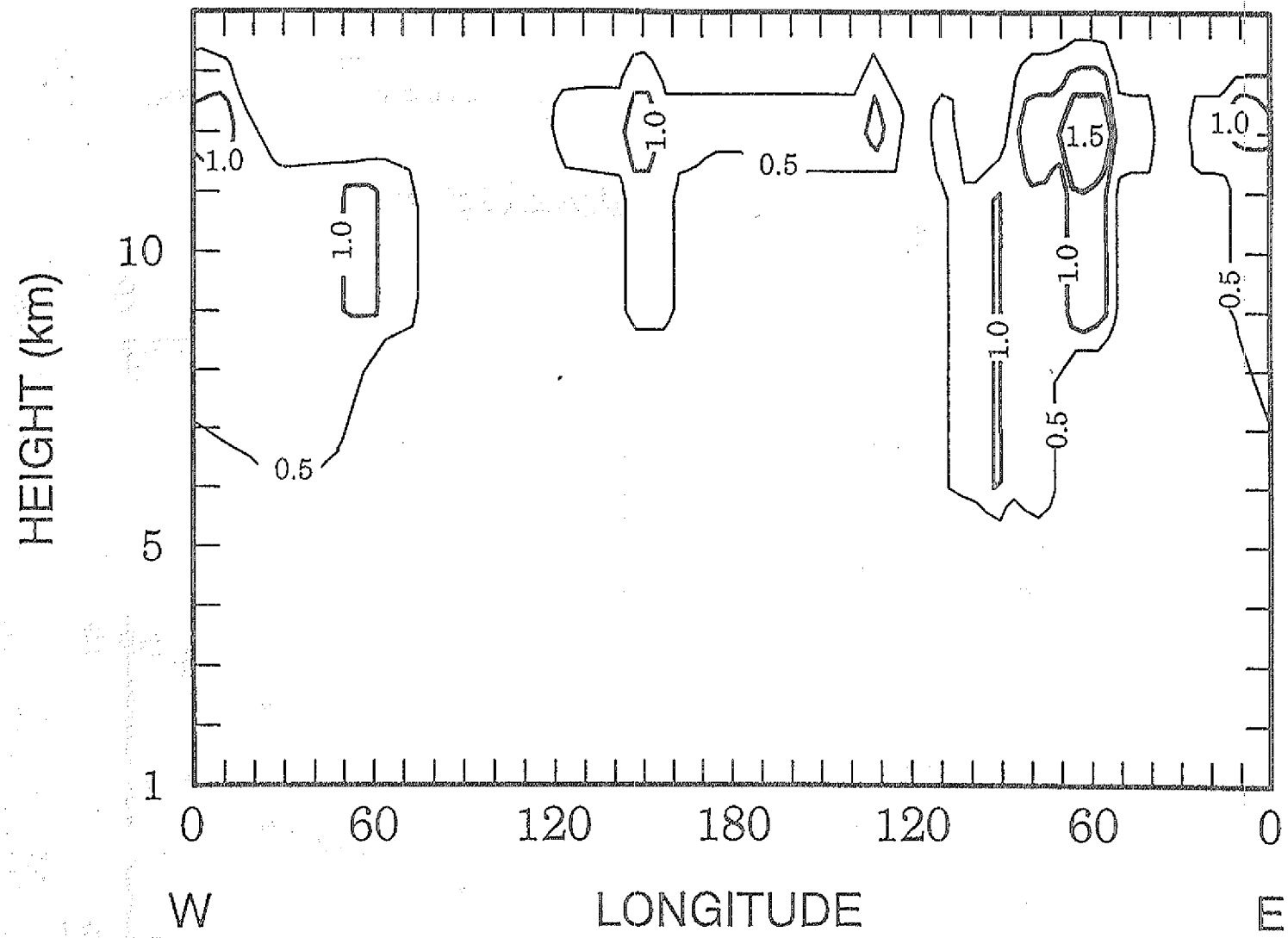

Figure 8 Contour plot of the zonal distribution of the NO_x emissions by aircraft at 40° to 50°N latitude. Contours shown at 0.5, 1.0, and 1.5 x 10^{11} molecules N $m^{-3}s^{-1}$.

3. RESULTS AND DISCUSSION

A model run is started at 0° longitude moving the air column in easterly direction. It is allowed to complete 3 cycles around the globe to ensure steady state. The latter is reached after 2 cycles: There is virtually no difference between the zonal NO_x distributions of the second and third cycle.

2-D Distributions and their Explanation

The zonal 2-D distributions of NO and NO_x resulting from the third cycle are displayed in Figures 9 and 10. They demonstrate that the salient features of the zonal NO and NO_x distribution are very similar. Firstly, in the boundary layer the respective concentrations exhibit a quick response to the surface sources. This is to be expected since the boundary layer is well mixed and the chemical life time of NO_x at low altitudes is quite short: Over the oceans the chemical life time of NO_x in the boundary layer averages about 10 hours mainly owing to the chemical removal of NO_2 via reaction (5) with OH (cf. Figure 5). The corresponding life time over the the continents is about 8 h, a little shorter because of the additional removal by dry deposition there. These are the characteristic times in which the boundary layer fills up with NO_x over the high source areas or is depleted to a new steady state when the air moves over terrain with no sources. Given the horizontal wind speed of 8 m s^{-1} the air column moves a characteristic distance of about 3° longitude in those times. This is short to the horizontal dimensions of the major surface source areas. As a consequence the isolines of the NO_x concentrations near the surface map closely the surface source strength.

As the high NO_x concentrations develop in the boundary layer over the high source areas, they become available for the fast upward transport by convective clouds. Indeed as Figures 9 and 10 show, the NO_x concentrations in the upper troposphere respond immediately with an increase when the air column moves over an area of high surface strength. As a consequence the troposphere over those areas is filled with NO_x from its upper as well as from its lower boundary.

In the upper troposphere, however, the chemical lifetime of NO_x is much longer than in the boundary layer - about 9 days at tropopause altitude. The high NO_x concentrations in the upper troposphere, therefore, increase and decay much more gradually than in the boundary layer. For the same reason the perturbations in NO_x induced in the upper troposphere by the surface sources spread much wider in longitude than they do in the boundary layer. Thus they become the most conspicuous features in the NO_x distributions. As Figure 9 and 10 indicate, NO_x introduced into the upper troposphere over Eastern North America reaches Europe, and the European injection of NO_x into the upper troposphere spread virtually all across the

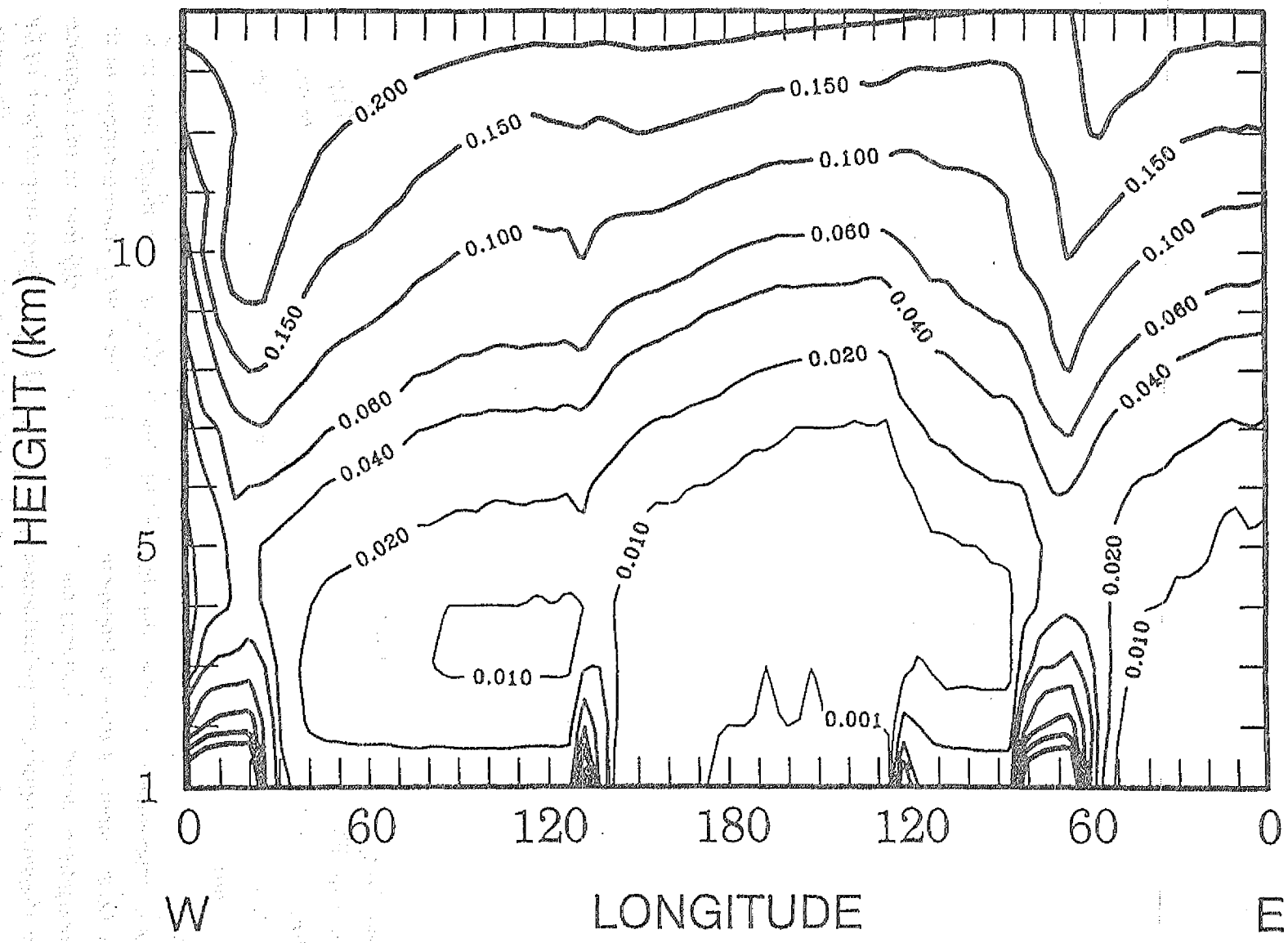

Figure 9 Contour plot of the zonal 2-D distribution of NO at 40°-50°N latitude. Contours in ppb at: 0.001, 0.01, 0.02, 0.04, 0.06, 0.1, 0.15, and 0.2.

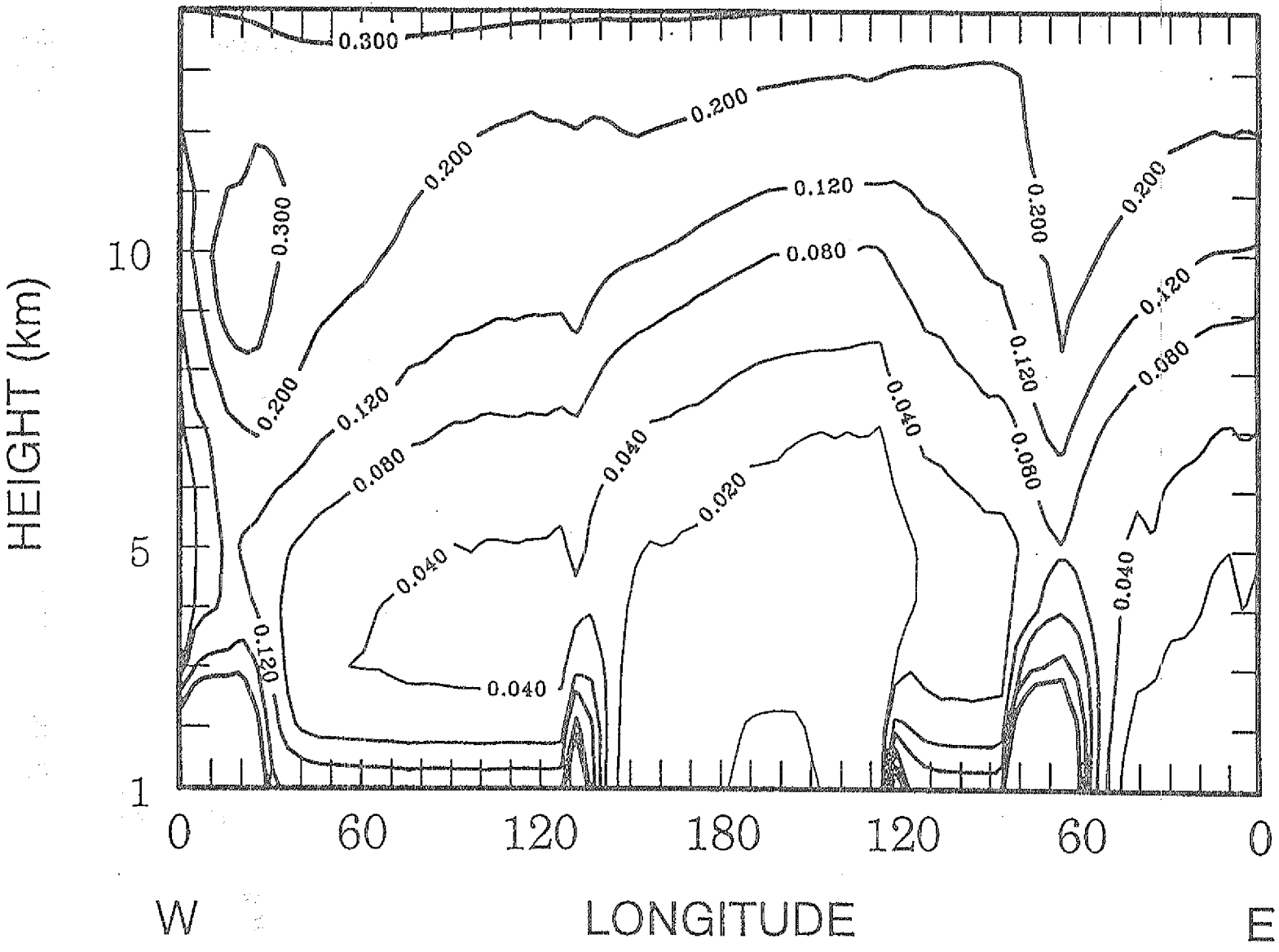

Figure 10 Contour plot of the zonal 2-D distribution of NO_x at 40°-50°N latitude. Contours in ppb at: 0.002, 0.02, 0.04, 0.08, 0.12, 0.2, and 0.3.

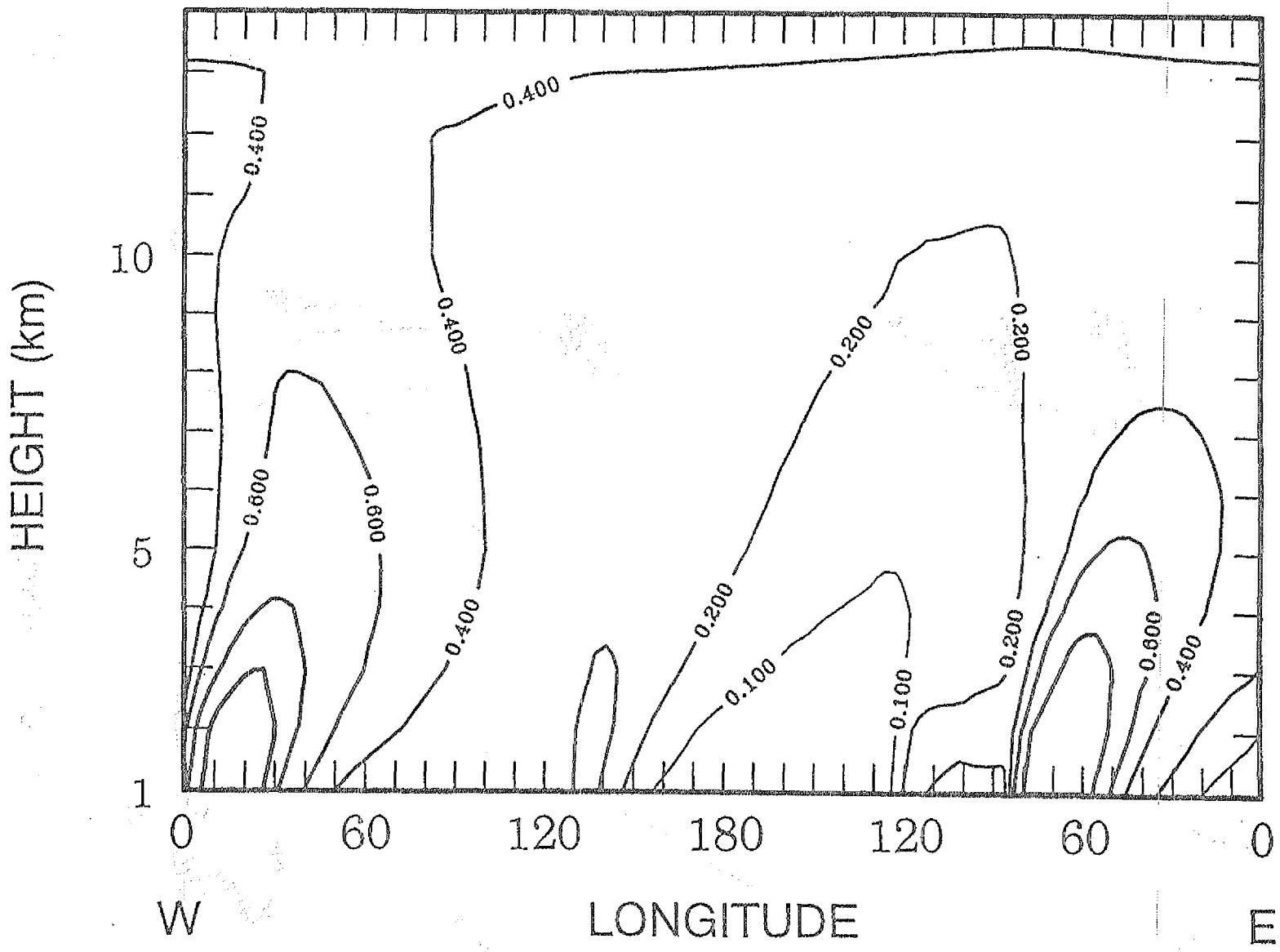

Figure 11 Contour plot of the zonal 2-D distribution of HNO_3 at 40°-50°N latitude. Contours in ppb at: 0.1, 0.2, 0.4, 0.6, 1.0, and 1.5.

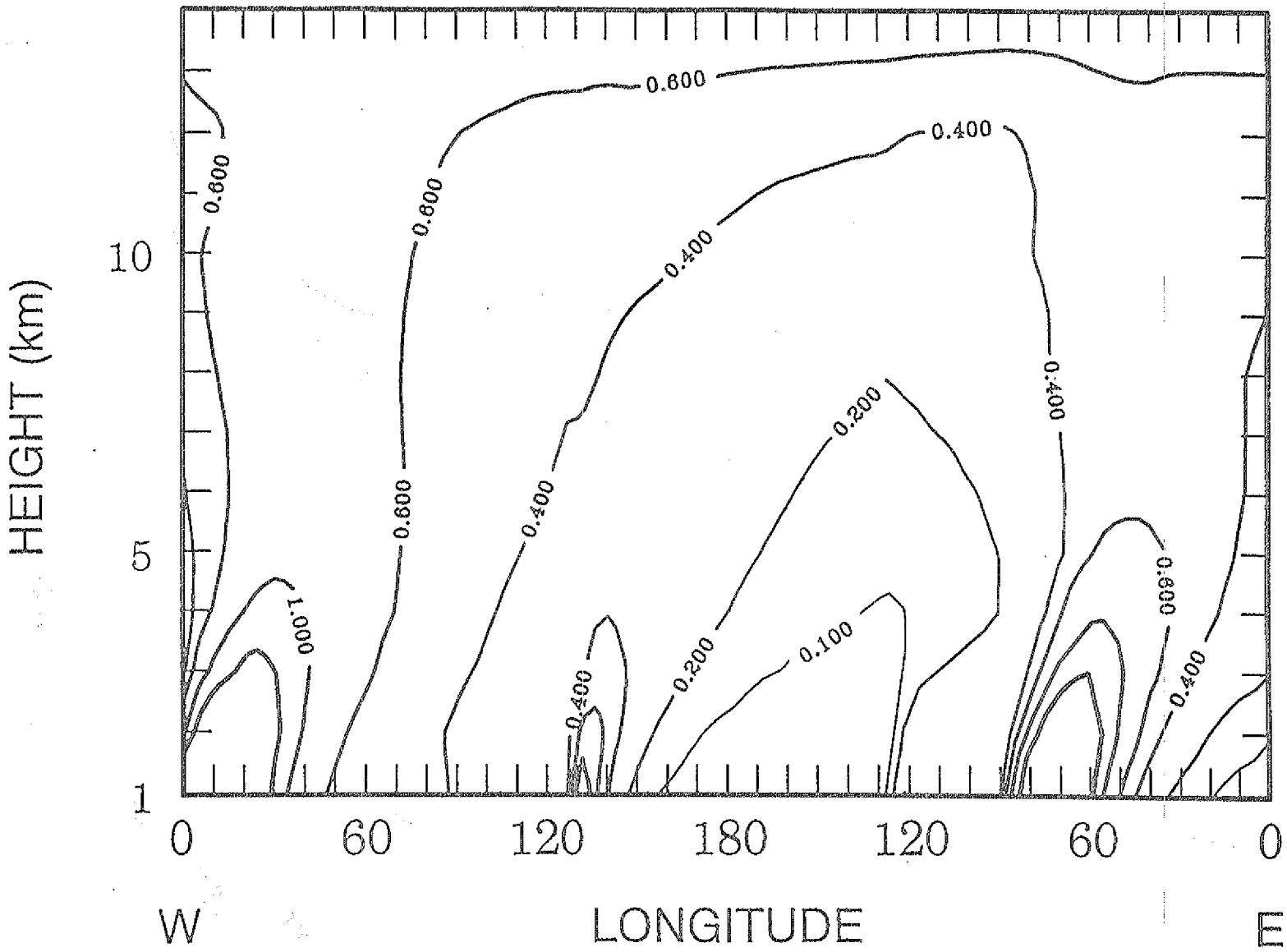

Figure 12 Contour plot of the zonal 2-D distribution of NO_y at 40°-50°N latitude. Contours in ppb at: 0.1, 0.2, 0.4, 0.6, 1.0, and 1.5.

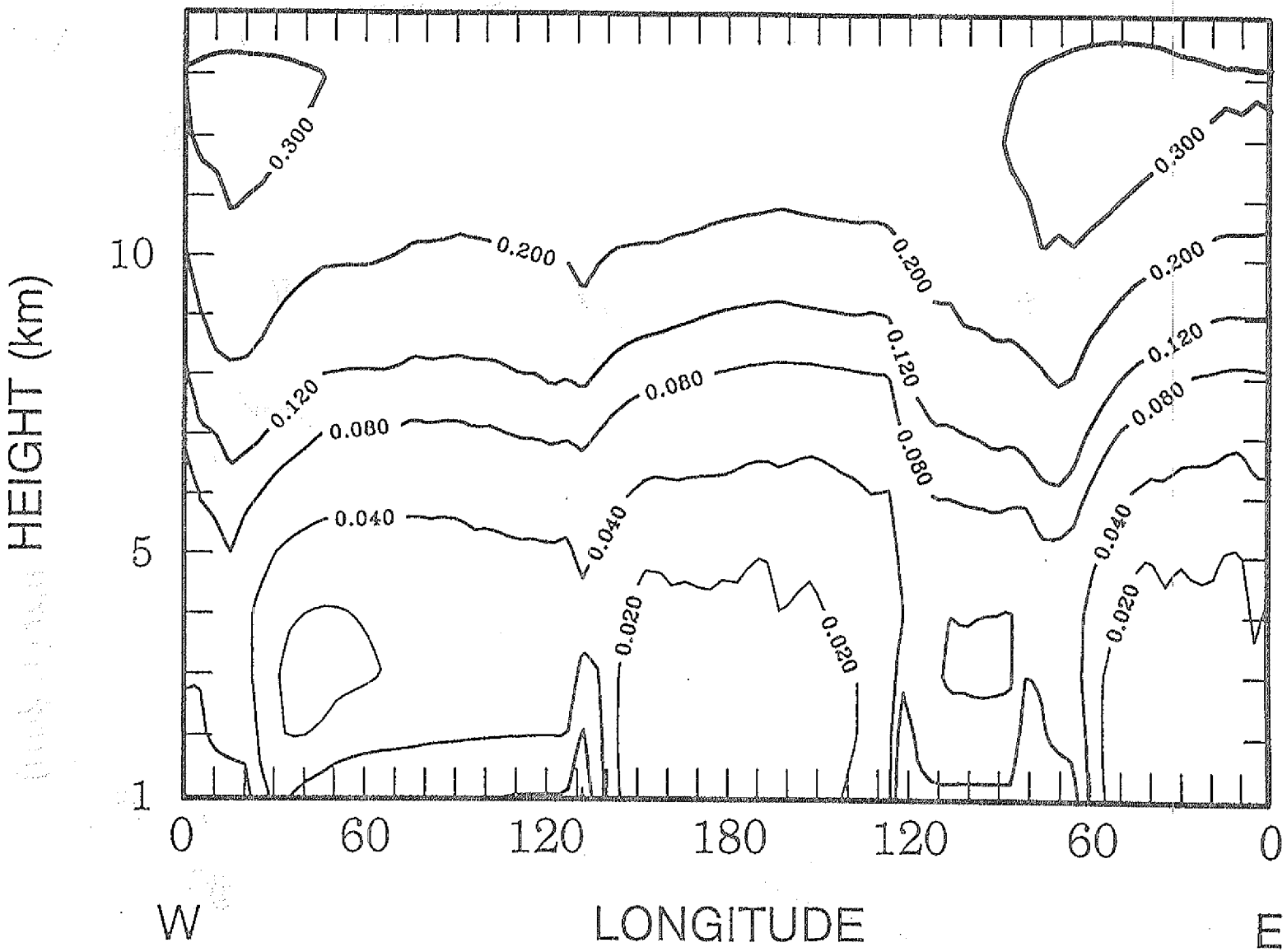

Figure 13 Contour plot of the zonal 2-D distribution of the [NO] / [NO_y] ratio at 40°-50°N latitude. Contours at: 0.02, 0.04, 0.08, 0.12, 0.2, and 0.3

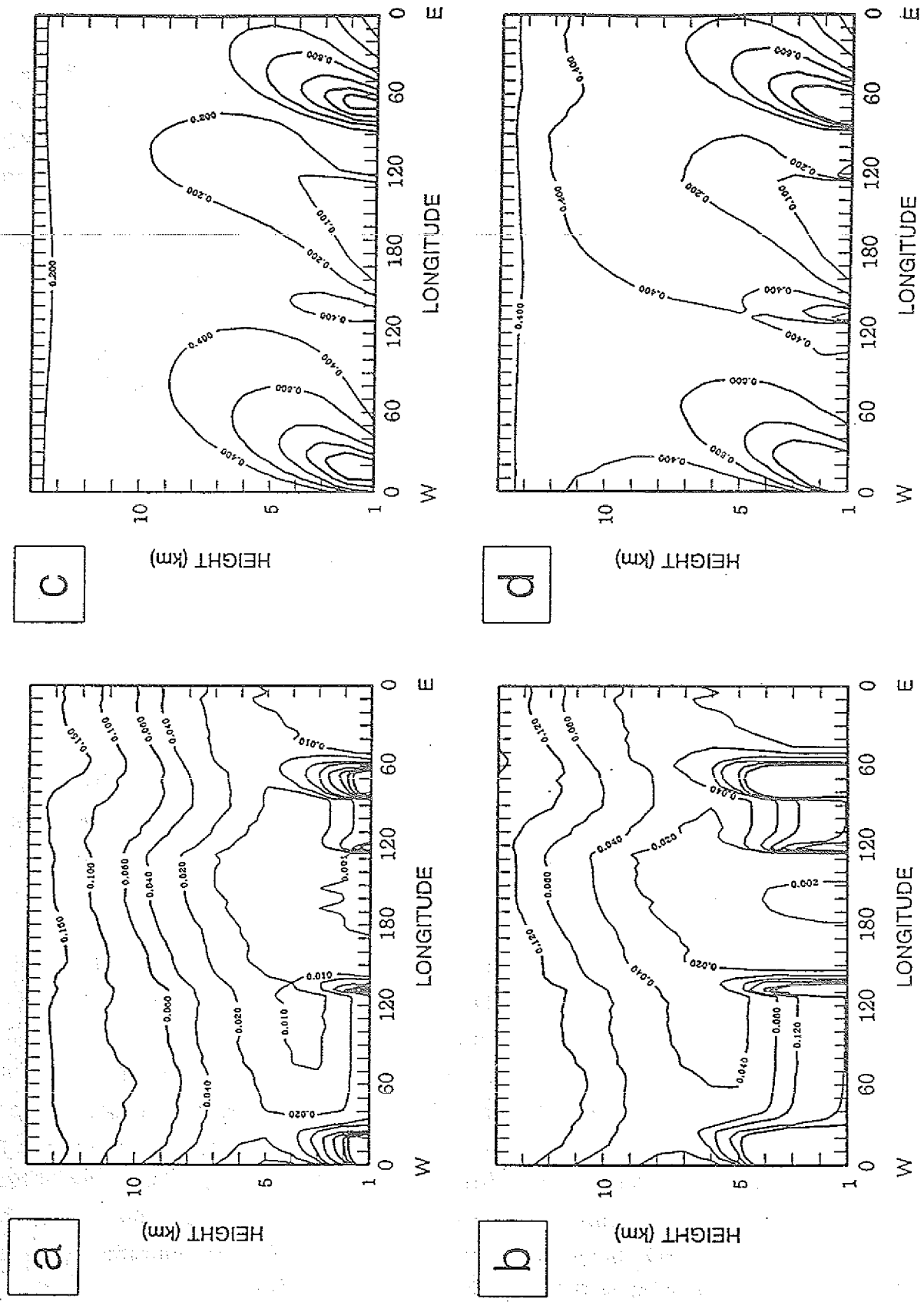

Figure 14 Contour plot of the zonal 2-D distribution at 40°-50°N latitude calculated with the fast vertical transport switched off. All contours in ppb.
Panel a: NO contours at: 0.001, 0.01, 0.02, 0.04, 0.06, 0.1, and 0.15.
Panel b: NO_x contours at 0.002, 0.02, 0.04, 0.08, 0.12, and 0.2.
Panel c: HNO_3 contours at: 0.1, 0.2, 0.4, 0.6, 1.0, and 1.5.
Panel d: NO_y contours at: 0.1, 0.2, 0.4, 0.6, 1.0, and 1.5.

Asian continent. Emissions by the Asian continent as whole reach North America. Figures 9 and 10 make it also clear that these perturbations reach well into the stratosphere. Over the areas perturbed by strong surface sources the model also predicts isolated maxima of the NO_x and NO in the upper troposphere, which are quite similar to those observed during STRATOZ III at 10 - 11 km altitude.

The fact that the pattern in the NO_x distribution in the upper troposphere is essentially caused by fast vertical transport can be seen from a comparison with the NO_x distribution from a model run in which the fast transport was switched off (see Figure 14).

That run shows much less structure in the NO_x distribution of the upper troposphere; the little structure that is left is an expression of the variations in the lightning and aircraft sources, whose distributions also tend to favor the continents. Even more important, the neglect of the fast vertical transport results in significantly lower NO_x concentrations in the upper troposphere at all longitudes.

Finally we note that in most parts of the zonal distribution field of Figure 9 the NO concentrations remain above 10 ppt. In all those parts atmospheric chemistry will produce O_3. Only the atmospheric regions enclosed by the 10 ppt isoline will produce little O_3 or even destroy it. These regions are mainly located over the oceans: Over the Pacific where the region extends from the surface to 7 km altitude and over the North Atlantic where it reaches to 5 km altitude. Minor isolated regions appear over the remote parts of the continents.

The model of course also generates the zonal 2-D distributions of HNO_3, and of $NO_y = NO + NO_2 + HNO_3$. They are shown in Figures 11, and 12, mainly for completeness. The model is intended to simulate the NO_x distribution in a reasonably realistic fashion. No such claim is made for HNO_3 or NO_y. Nevertheless, those distributions will also be discussed briefly.

HNO_3 exhibits a 2-D distribution pattern quite different from those of NO and NO_2. This is not too surprising because it has a physico-chemical behaviour quite different from that of the NO_x species. HNO_3 is not emitted into the atmosphere by external sources, but is formed in the atmosphere from the conversion of NO_2 mainly via reaction (5). As we have seen this conversion is fast in the lower troposphere and slow in the upper troposphere (see Figure 5). Nevertheless, even with the fast conversion the build up of the HNO_3 concentration in the boundary layer over the areas of strong surface sources is delayed with respect to that of NO_x. The maximum of the HNO_3 concentration is only reached after 20° in longitude rather than after 3° as in the case of NO_x. Similarly, the decay of the high HNO_3 concentrations trails that of the NO_x by a distance of about 30° longitude (see also Figure 16).

In addition transport of HNO_3 into the upper troposphere by convectice clouds is greatly diminished because in-cloud scavenging removes half of the HNO_3 as the air parcel is lofted. The increase of HNO_3 in the upper troposphere over strong surface sources is therefore weak and barely visible in Figure 11. The fact that most of the HNO_3 is formed in the lower

troposphere, and that its lifetime against rainout in the free troposphere is relatively long, about 10 days, tends to concentrate the high HNO_3 mixing ratios in a plume slanted downwind in the wake of the strong surface sources and reaching into the middle troposphere. Because of its long life time HNO_3 is also the major NO_y component, and its distribution features dominate the zonal concentration pattern of NO_y in Figure 12. A comparison with Figure 14 shows that in contrast to NO_x the neglection of the fast vertical transport does not change much the basic pattern of the zonal distributions of HNO_3 and NO_y. Without fast transport, however, the plumes are more slanted and do not reach as high. There is also a tendency of lower NO_y concentrations in the upper troposphere. Because NO and NO_y are the most commonly measured oxidized nitrogen compounds in the free troposphere, we add a zonal plot of the model calculated NO/NO_y ratio to facilitate future comparison (Figure 13).

The contribution of the different sources

To identify the contribution of the various sources to the tropospheric NO_x distribution, we performed a number of model runs in which each of the individual sources was switched off - one at a time. The resulting changes in the NO_x distribution are difficult to see when using the 2-D zonal plots presented so far, except for the ground source which causes a large impact. The other sources are too evenly distributed to cause a clearly visible change in pattern. To demonstrate the respective contributions more quantitatively, we present the NO_x and HNO_3 data in form of vertical concentration profiles. We selected two sequences of profiles: One leading in 5° steps from a high surface source area out over the ocean and one leading from the ocean over a high surface source, i.e. the coastal waters of Eastern North America, and the continental Western Europe for which profile measurements of NO are available. Each of the calculated vertical profiles provides a breakdown of the contributions from the individual sources.

Figure 15 demonstrates that all 4 sources contribute significantly to the NO_x content of the upper troposphere over the western Atlantic. In that region, where air traffic is heavy, emissions by air craft provide the single most important contribution. It amounts to up to 40 % of the total. Even over the Atlantic, however, the next largest contribution of NO_x, about 35 %, comes from the continental surface source. The remainder is shared by the stratospheric and lightning sources. The contributions from aircraft, lightning and stratospheric input taper off with decreasing altitude. The NO_x concentration in the middle and lower troposphere is dominated by the continental ground source. Figure 15 also shows the development of the vertical profiles of the NO and NO_x concentration as the air moves out over the Atlantic.

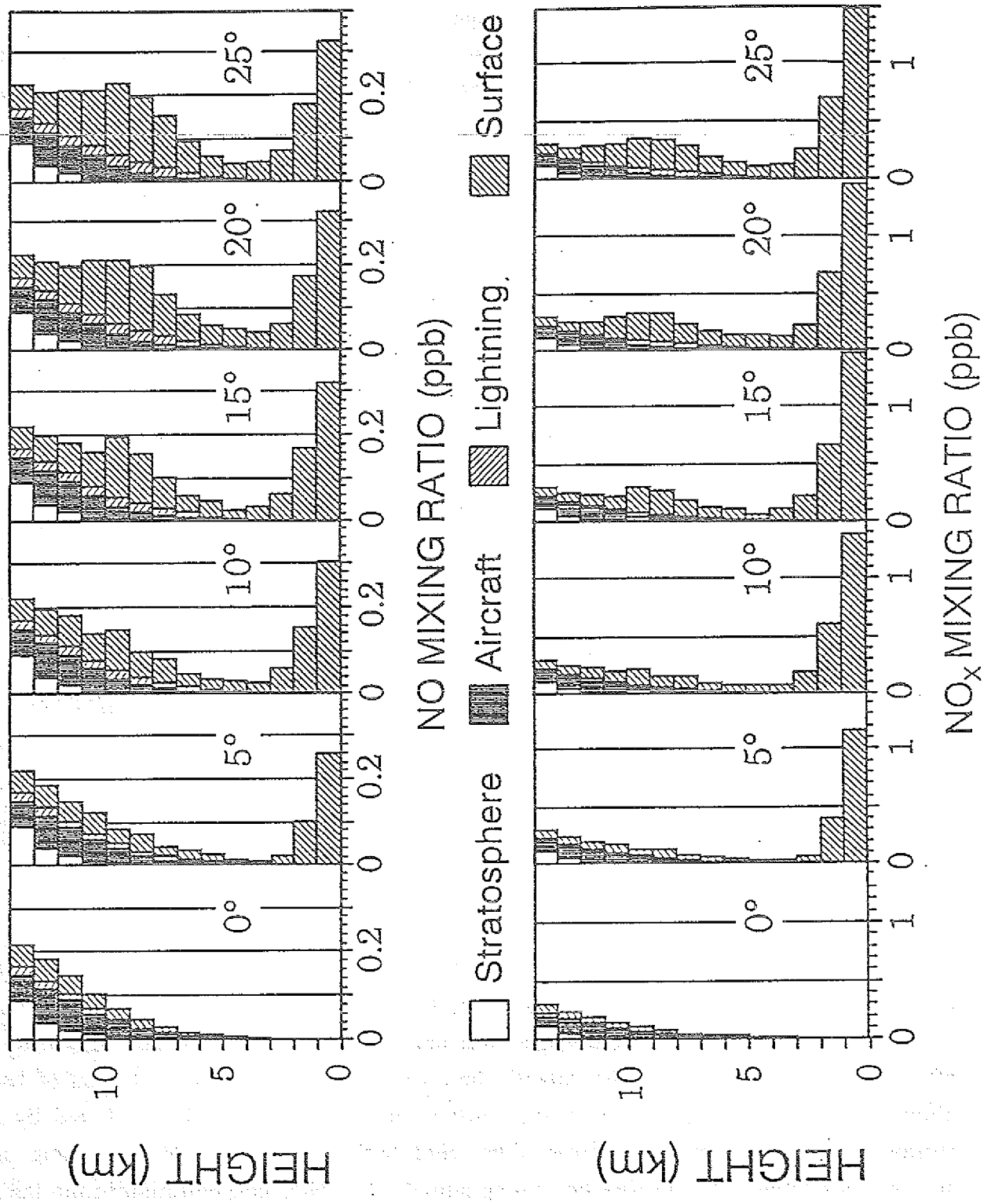

Figure 15 Vertical mixing ratio profiles of NO (top panel) and NO_x (bottom panel) over the Western North Atlantic. The different shadings indicate the contributions from the individual source.

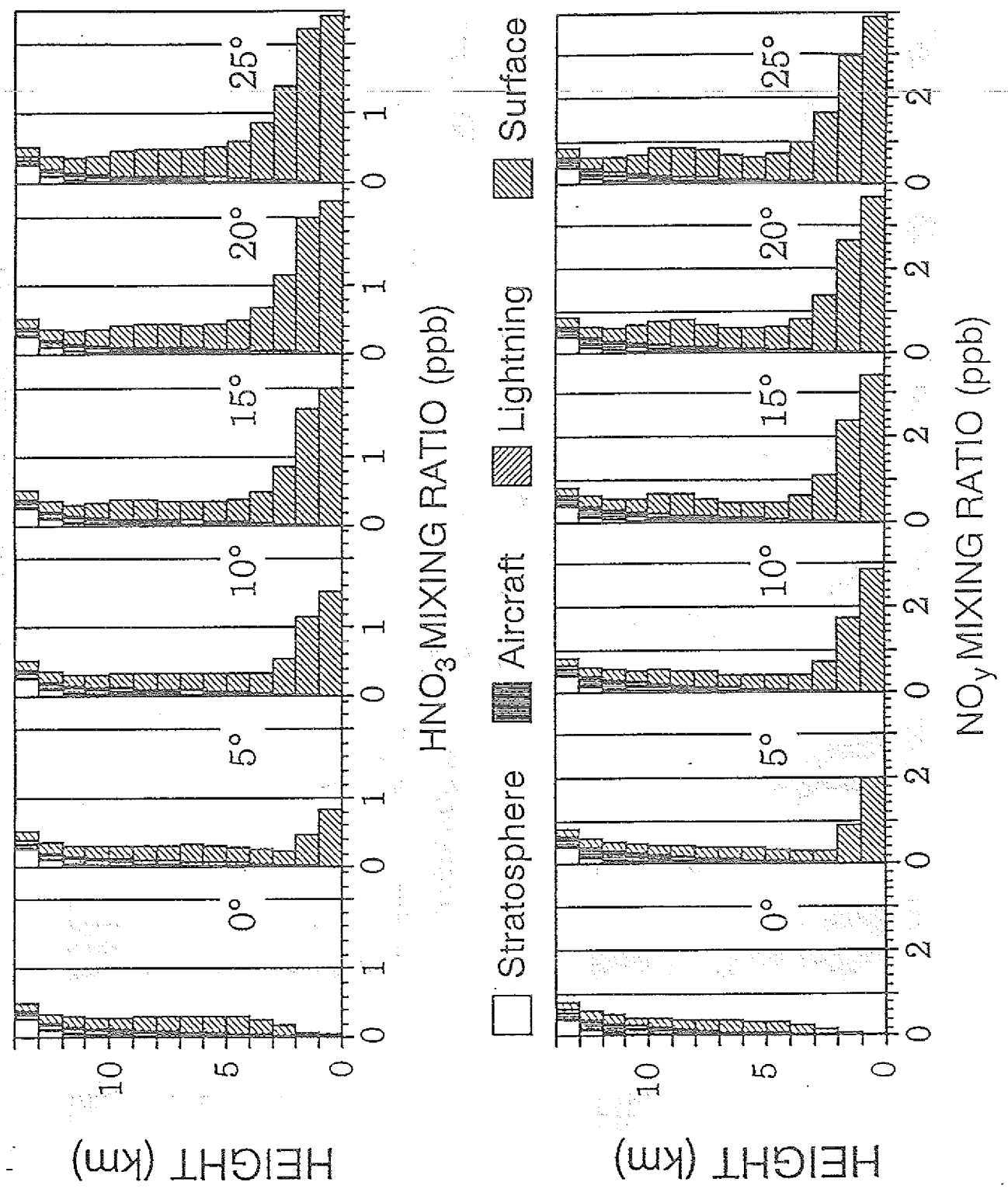

Figure 16 Vertical mixing ratio profiles of HNO_3 (top panel) and NO_y (bottom panel) over the Western North Atlantic. The different shadings indicate the contributions from the individual sources.

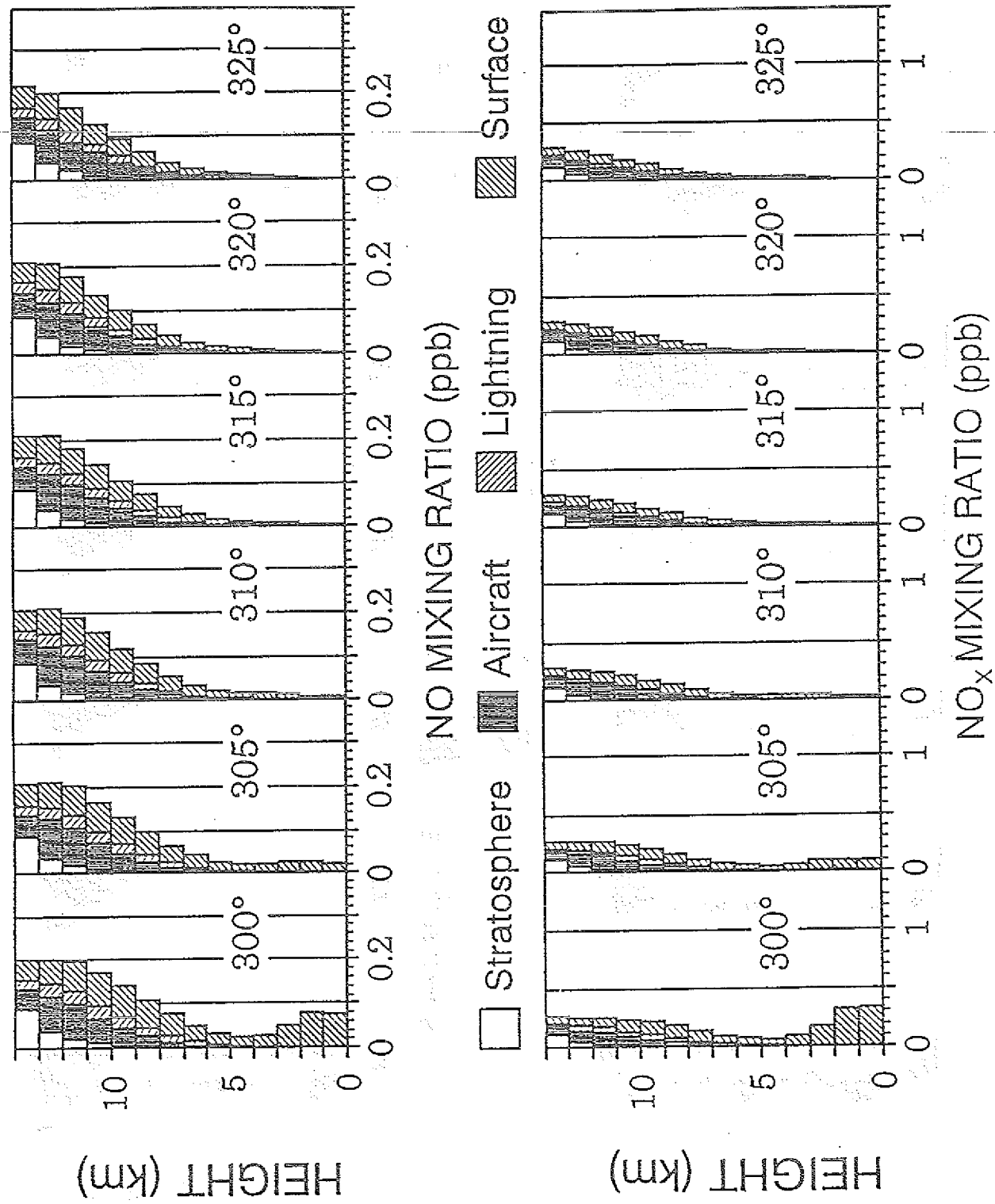

Figure 17 Vertical mixing ratio profiles of NO (top panel) and NO_x (bottom panel) over continental Western Europe. The different shadings indicate the contributions from the individual sources.

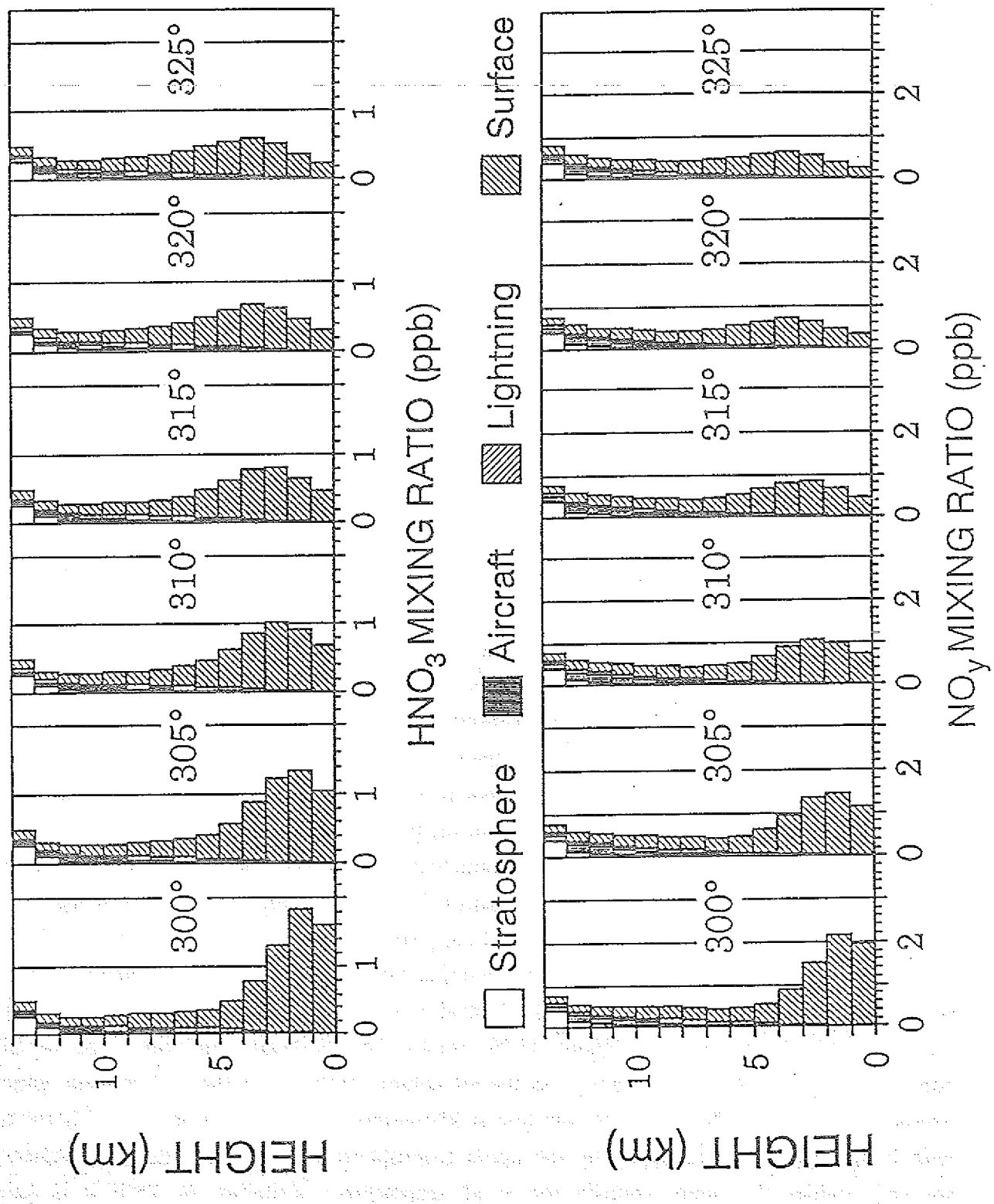

Figure 18 Vertical mixing ratio profiles of HNO_3 (top panel) and NO_y (bottom panel) over continental Western Europe. The different shadings indicate the contribution from the individual sources.

Owing to its rapid conversion to HNO_3 the NO_x concentration in the middle and lower troposphere decay quickly with increasing distance from the surface source which ends at 65°W longitude.

On the other hand the NO and NO_x concentration in the upper troposphere change relatively little. This is the combined effect of the long chemical lifetime of NO_x and the continued input from the stratosphere and aircraft emissions. Both effects produce oceanic profiles of NO and NO_x with a strong vertical increase in the upper troposphere.

The corresponding profiles of HNO_3 and NO_y are presented in Figure 16. Again all sources contribute significantly to the HNO_3 content of the upper troposphere, but the relative weights are different from those for NO_x. The contribution by the ground sources dominates at all altitudes, even in the upper troposphere.

There are two reasons for this. Due to the relatively long life time of HNO_3 in the free troposphere its vertical profile accumulates contributions from the continental surface sources over a longer time period. Secondly, the aircraft emissions which are exclusively in the form of NO_x, trigger an immediate response in the NO and NO_x profile but a delayed one in the HNO_3 profile, since the conversion of NO_2 to HNO_3 in the upper troposphere is slow.

Comparison of Figures 15 and 16 emphasizes the difference in the distributions of NO_x and HNO_3 already indicated in the 2-D zonal distributions of Figures 9 and 11. When the air column moves away from a strong surface source, the vertical profile of the HNO_3 concentration is dominated by transport processes, because the chemical lifetime of HNO_3 is long. Dry deposition and below-cloud scavenging erode its profile from below, and upward transport by eddy diffusion spreads the high HNO_3 concentration in the lower troposphere slowly upward. This results in a HNO_3 concentration maximum at low altitudes which flattens but increases in altitude with increasing downwind distance from the surface source.

The vertical NO_y profiles in Figure 16 represent essentially the average of the NO_x and HNO_3 profiles which to some extent washes out the prominent features of the NO_x profiles.

Figures 17 and 18 show the inverse process, namely the filling up of the troposphere with NO_x and NO_y over a strong extended surface source. The air column arriving in Europe after crossing the Atlantic shows very low NO and NO_x concentrations in the lower troposphere. But it still carries large amounts of NO_x in the upper troposphere, in fact at 0° longitude there is still a significant contribution, about 30 %, from the North American surface sources. The largest contribution, however, about 45 %, comes from aircraft emissions, due to the continued input accross the Atlantic. As the air column moves over the source area, which extends from 0° to 25°E longitude, the lowest kilometers of the troposphere quickly fill up with NO_x followed more slowly by the upper troposphere. By 10°E longitude the surface source provides the major contribution at all tropospheric altitudes, by 25°E it is quite dominant. Aircraft emissions maintain their share in absolute terms, but decrease to about 25 % in the upper troposphere at 25°E longitude on a relative basis.

Figure 17 not only shows quantitatively how the troposphere fills with NO_x from its upper and lower boundary, it also demonstrates the development of a maximum in NO and NO_x concentrations at 10 km altitude as the air column passes over the source area. The breakdown into the contributions from the different sources makes it clear that the maximum is a result of high surface concentrations carried upward by the fast transport. All the other sources together would only generate a monotonic increase in NO and NO_x in the upper troposphere. The maximum is more clearly expressed in the vertical profiles of the NO_x mixing ratio. The difference is due to the fact that the decrease of the NO_x profile with altitude is partly compensated by the increase in the NO/NO_2 ratio. The vertical gradient in the NO/NO_x ratio is also responsible for the relatively large concentrations of NO in the upper troposphere with respect to its concentrations in the lower troposphere.
The result is a nearly C-shaped vertical profile of the NO concentration over a region with strong surface sources.
Figure 18 reemphasizes that build-up of the tropospheric HNO_3 profile proceeds mainly from the lower boundary. The NO_y profile just barely maintains a concentration maximum in the upper troposphere.

Comparison with experimental data and results from other models

The results presented so far make a number of quite specific predictions about the vertical distribution of NO, NO_x and HNO_3, which can be tested - at least in principle - against experimental results. Unfortunately, only few data are available in the literature for such a comparison.
As mentioned before the NO measurements by Drummond et al., 1988, summarized in Figure 1 represent a large share of the available NO_x measurements in the upper troposphere, and as indicated at several points in the discussion before the model appears to describe quite well the general features of the observed vertical NO distribution in the upper troposphere over the coastal zones. Figure 19 presents a more detailed comparison for the NO profile off the coast from North America. The experimental data represent an average of the NO measurements between 50°N and 40°N latitude along the south bound leg of STRATOZ III (Drummond et al., 1988). The average profile was preferred over an individual one for better correspondence to the climatologically averaged NO profiles generated by our model. The calculated profile (full curve) is that for 50°W longitude from Figure 15.
The two profiles agree surprisingly well, although the experimental profile indicates a maximum at 10.5 km altitude which is not reproduced by the model. This agreement is all the more gratifying as no attempt had been made to tune any of the model parameters to better

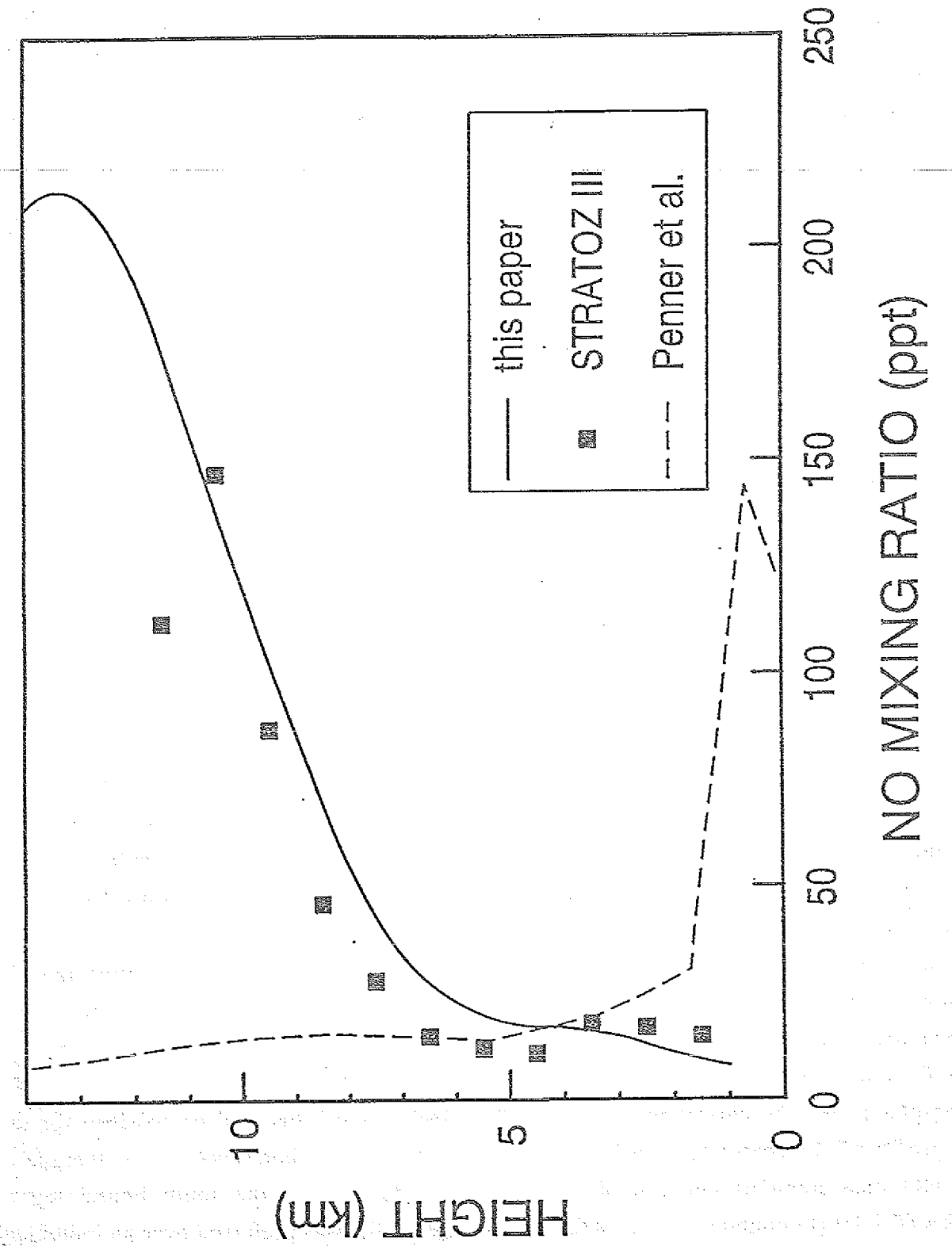

Figure 19 Vertical profiles of the NO mixing ratio over the East coast of North America. Solid line: model calculation 50°W longitude (this paper); closed squares: averaged measurements between 50°W and 40°N latitude along the south bound leg of STRATOZ III [Drummond et al., 1988]; dashed line: 3-D model calculation for 45°N, 63°W by Penner et al., 1991.

match the empirical profiles. It also indicates that all four sources are needed to produce the high NO concentrations in the upper troposphere. For further comparison Figure 19 includes a NO profile calculated for 45°N, 63°W by a 3-D model (Penner et al., 1991). This profile deviates considerably from the NO concentrations measured in the upper troposphere. The reason is that the two sources which according to our model are mainly responsible for the high NO in the upper troposphere, namely aircraft emissions and fast upward transport from the boundary layer, are not treated in that 3-D model: Aircraft emissions are not included at all, and convective transport is parameterized by exchange between adjacent altitude levels only, which does not allow the direct displacement of boundary layer air into the upper troposphere. In fact the NO concentrations predicted by that model in the upper troposphere are barely compatible to those caused by stratospheric input alone in our model (cf. Figure 15).

The lack of fast transport accounts also for the inability of that model to reproduce the high NO concentrations observed in the upper troposphere at lower latitudes (see Figures 14 to 15 by Penner et al., 1991), whereas preliminary runs with our model show that biomass burning or lightning, which is much more important at low latitudes, suffice to generate such concentrations over much of the continental tropics.

There are a few additional model predicted quantities which might be of diagnostic value and helpful for comparison with other models. One example are the longitudinal profiles of dry and wet deposition rates given in Figure 6, whose integrated values are given in Table 2. Comparison of the total latitudinal emission rate with the total deposition rate, which both equal 9.0×10^6 tN/yr indicates that NO_y is conserved in the model.

Wet deposition can also be tested regionally. For Northamerica (120°E - 0°E) our model predicts an average wet deposition rate of 15.3 kgN/km^2/month. This can be compared to the wet deposition rates given in Figures 22a and 22c by Penner et al. [1991], from which we extract a mean measured rate of 19 kgN/km^2/month, and 9.5 kgN/km^2/month predicted by their model for the month of July.

Another informative quantity is the NO_y flux leaving the boundary layer by fast vertical transport. It amounts to 15 % of the total surface emissions, but only 2 % of the surface emissions reach the upper troposphere. The model calculates an average tropospheric burden of 1.6×10^4 tN for NO_x and of 4.7×10^4 tN for HNO_3. The corresponding tropospheric lifetimes in June at 40°-50° latitude are 0.6 day for NO_x and 2.1 days for HNO_3. The residence times in the planetary boundary layer, which result from the combined action of chemical reactions, dry and wet deposition and upward transport, are 6 h for NO_x and 14 h for NO_y.

Table 2

Model average deposition rates of NO_x and HNO_3 in June 1984 at 40°-50°N latitude

Deposition process	HNO_3 (10^6 tN/yr)	(%)	NO_2 (10^6 tN/yr)	(%)
dry deposition (continents)	3.46	38.3	1.25	13.8
dry deposition (oceans)	0.94	10.4	0.00	0.0
dry deposition (total)	4.40	48.7	1.25	13.8
wet deposition in cloud (continents)	0.63	7.0	0.00	0.0
wet deposition below and entrainments (continents)	1.88	20.8	0.00	0.0
wet deposition in cloud (oceans)	0.12	1.3	0.00	0.0
wet deposition below and entrainment (oceans)	0.77	8.5	0.00	0.0
wet deposition (total)	3.40	37.6	0.00	0.0
total deposition (NO_2 + HNO_3)		9.05		100.2
total emission		9.03		100.0

The role of aircraft emissions

One of the intentions of this paper is to demonstrate the importance of aircraft emissions in the NO_x budget of the upper troposphere. Figures 15 and 17 showed that over the North Atlantic and Europe i.e. close to the major flight corridors about 40 % of the NO_x in the upper troposphere come from aircraft. But because of aircraft injection at other longitudes (see Figure 8), strong zonal winds and the long lifetime of NO_x in the upper troposphere, the impact of aircraft emissions is significant all around the 40°N to 50°N latitude band. The zonally averaged contribution to the NO_x budget of the upper troposphere is 30 %. The lowest contribution occurs over eastern Asia with about 15 %. Although a weak source globally, aircraft emissions make a major contribution in the upper troposphere at 40°N to 50°N latitude due to their singular injection pattern. This is also true for the other northern midlatitudes.

Some of that influence extends upward into the lower stratosphere - partly because of some direct emissions, but mostly by upward transport through eddy diffusion, which in the real world may be counteracted by mean downward motion.

It is important to note that our calculations were made for 1984. Since that time air traffic has been increasing at a rate of 7 % per year, such that today's emissions by the commercial air fleet are nearly 50 % higher than those used in the model. Since our model uses prescribed OH and O_3 profiles, an increase in NO_x does not couple back to produce a change in the chemical lifetime of NO_x. Thus our model responds with a linear increase in NO_x concentrations to an increase of any source, as long as the geographical emission pattern does not change. As a consequence the model would predict an contribution by air craft emissions for 1991 which is higher by 50 % in absolute terms than those shown in Figures 15 and 17. The relative zonal contribution in the upper troposphere would increase to about 40 %. Presumably the anthropogenic surface sources have increased also. But their rate of increase is expected to be much slower, around 1 %/yr, than that of the aircraft emission. Unless climatic changes induced a higher convective activity, most of the expected increase in NO_x concentrations in the upper troposphere at midlatitudes would be due to increased air traffic.

The validity of model simplifications

Finally we address the question whether our simplified model simulates properly the mechanisms essential for generating the high NO_x concentrations observed in the upper troposphere or whether improving on any of the simplifications would so drastically change the predicted NO_x distribution as to invalidate our results. We first deal with the limitations in chemistry. Clearly the list of NO_y compounds is very incomplete; two of the most abundant

NO_y species namely peroxyacetylnitrate, PAN, and nitrate aerosol NO_3^-, are not treated. As far as NO_x is concerned this is not a serious shortcoming. In summer the concentration of PAN is low. The measurements of Rudolph et al. [1987] during STRATOZ III gave PAN concentrations around 0.05 ppb at 40°N to 50°N latitude. Thus PAN contributes little to NO_y and can be safely neglected. Moreover the chemical conversion of HNO_3 and NO_3^- back to NO_x is slow compared to the physical removal of these compounds by rainout and dry deposition such that the sensitivity of the modelled NO_x distribution to the treatment of HNO_3 and NO_3^- is quite small. Consequently the neglect of nitrate aerosol has little impact on the calculated NO_x distributions. In fact NO_3^- can be considered as implicitly included in the HNO_3 distributions because the tropospheric fate of the nitrate aerosol is quite similar to that of HNO_3. Thus, since PAN is low, even our NO_y distributions should not be affected much by the incomplete treatment of NO_y species. This is of course not true for the distribution of HNO_3.

Much more important for the NO_x distribution is the current lack in the quantitative understanding of the fate of the NO_3 radical in the free troposphere. Its various homogeneous and heterogeneous conversion rates to NO_3^- are difficult to parameterize because the distributions of the reaction partners are poorly known. This is, of course, a difficulty for any model. In summer when reaction of NO_2 with OH is fast, and dominates the conversion of NO_x to HNO_3, this lack is expected to cause a relatively small uncertainty. In winter, however, when the reaction with OH is slow, the reaction via the NO_3 radical will determine the chemical lifetime of NO_x in the troposphere, and thus impact strongly on the NO_x distribution.
For the summertime treated here, however, our simplified chemical scheme should provide a reasonably realistic representation of the NO_x chemistry in the free troposphere.

The representation especially of the horizontal transport in the model cannot claim to be realistic even in a climatological sense: It totally neglects meridional transport. The vertical shear in the zonal wind is also neglected and so is the zonal eddy diffusion. Any of these factors will directly influence the NO_x distribution - but not to a degree that would seriously alter the salient features derived from our simple model, namely the high NO concentrations in the upper troposphere and the relative size of the contributions from the various sources.
The meridional transport which is essentially in the form of eddies, will dilute the NO_x concentrations in the upper troposphere to some extent. Its main effect will be to eventually spread the plume from the anthropogenic surface sources and aircraft emissions over a wider band of latitudes. The other sources including microbial emission of NO at the continental surfaces are less confined in latitude and provide less of an meridional gradient on which the horizontal transport could act. However, even the anthropogenic surface sources range over 20° to 30° latitude. Within the lifetime of NO_x the meridional eddy diffusivity which is around

2×10^6 m^2s^{-1} [Murgatroyd, 1969] will cause the plumes in the upper troposphere to expand by about 10° latitude. This causes a dilution of about 30 %, certainly a significant effect, but smaller than the uncertainties in the source strengths given in the previous section.

Zonal eddy transport whose diffusivity is of a similar magnitude as the meridional one has to compete with the mean zonal wind. Thus its impact is even less. Its effect will be visible mainly in the upwind propagation of the signal from the strong surface sources by about 3° longitude.

The neglect of the vertical shear in the zonal wind will introduce some changes in the 2-D distribution of NO_x - mainly in the upper troposphere. As we have seen the lifetime of NO_x at lower altitudes is quite short. As a consequence high boundary layer concentrations of NO_x can only be maintained close to the strong surface sources and the NO_x isopleths in the lower troposphere will be virtually the same for all realistic surface wind speeds. By the same token the injection of NO_x into the upper troposphere by fast vertical transport will remain at the same range of longitudes.

In the upper troposphere the transport by zonal wind is of course important and a realistic mean wind speed of 15 ms^{-1} in the upper troposphere which is twice as large as the vertically uniform wind speed of 8 ms^{-1} assumed in our model would spread the high NO_x concentration injected from below over twice the distance. Also the effect of the atmospheric NO_x sources by lightning and aircraft emissions which are stronger over the continents would be spread more evenly resulting in smoother NO_x contours in the upper troposphere. But the prediction of NO_x concentrations in the upper troposphere much higher than those expected from stratospheric input alone remains valid. Moreover, since the injection rate of NO_x into the upper troposphere from the ground source or from any of the other sources is not changed by our simplifications the predicted relative importance of those sources remains valid also - at least for the zonal average.

4. CONCLUSION

In the foregoing we presented a simple model to simulate the 2-D NO_x distribution in a zonal belt. Because of its simplicity the model is easy to operate: a run takes 20 min. on a PC 486 Computer. For the same reason its results are easy to understand and allow to identify those processes that dominate the NO_x distribution as well as those which cause the highest uncertainties. Despite of its simplicity the model is capable of reproducing the salient features of the zonal NO_x distribution. In particular it reproduces the high values and relative maxima of the vertical NO profiles in the upper troposphere over coastal areas. For the simulation of these maxima fast and direct upward transport of air from the boundary layer proved necessary.

The model facilitates a first examination of the contributions from the various sources to the NO_x concentration in the upper troposphere: Stratospheric input is significant but not dominant. Aircraft emissions which contribute on average about 30 % and NO_x lofted from the planetary boundary layer are the major sources of NO_x in the upper troposphere at northern midlatitudes during summer. (In the continental tropics lightning coupled to fast vertical transport appears to be the major factor). The quantitative conclusions are of course uncertain. They depend on the assumed source strengths which have errors on the order of a factor of 2. These errors propagate into errors of also a factor of 2 in the respective absolute contributions to the composite vertical NO_x profiles, since the NO_x concentrations predicted by the model respond linearly to the source strenghts.

For the same reason these NO_x profiles can easily by corrected once the true source strenghts are known by appropriate scaling of the respective contributions.

The model can also be applied to other latitudes and seasons. Before doing so we would like to introduce some improvements to ensure applicability. Such work is in progress.

REFERENCES

Attmannspacher, W., R. Hartmannsgruber, and P. Lang, Langzeittendenzen des Ozons der Atmosphaere aufgrund der 1967 begonnenen Ozon Messreihen am meteoroloischen Observatorium Hohenpeissenberg, Meteorol. Rdsch., 37, 193-199, 1984.

Boettger, A., D. H. Ehhalt and G. Gravenhorst, Atmosphaerische Kreislaeufe von Stickoxiden und Ammoniak, in Juel - Bericht, vol. 1558 KFA Juelich, Juelich, 1978.

CIAP, /Climatic Impact Assesment Program 1975, Propulsion effluent in the stratosphere, Monograph 2, U.S. Department of Tranportation report DOT-TST-75-52, Washington, D.C., 1975.

Drummond, J. W., D. H. Ehhalt, and A. Volz, Measurements of nitric oxide between 0-12km altitude and 67oN - 60oS latitude obtained during STRATOZ III, J. Geophys. Res., 93, 15,831-15,849, 1988.

Ehhalt, D. H. and J. W. Drummond, The tropospheric cycle of NOx: Chem. Unpoll. Poll. Troposphere, in Proc. NATO Adv. Study Inst., Corfu, Greece, 28 Sept.-10 Oct., 1981, pp. 219-251, edited by H. W. Georgii and G. Jäschke Reidel, Dordrecht(NL), 1982.

Ehhalt, D. H. and J. W. Drummond, NOx sources and the tropospheric distribution of NOx during STRATOZ III, in Tropospheric Ozone, pp 217-237, edited by I. S. A. Isaksen Reidel, Dordrecht(NL), 1988.

Ehhalt, D. H., Vertical profiles of NO in the free troposphere based on STRATOZ III, in: Extended Abstracts of the Second Conference on the Scientific Application of Baseline Observations of Atmospheric Composition, Aspendale, Australia, 14-17 November 1988, p. 33.

Ehhalt, D. H., J. Rudolph, F. Meixner, and U. Schmidt, Measurements of selected C2-C5 hydrocarbons in the background troposphere: Vertical and latitudinal variations, J. Atmos. Chem., 3, 29-52, 1985.

Gidel, L. T., Cumulus cloud transport of transient tracers, J. Geophys. Res., 88, 6587-6599, 1983.

Hameed, S., and J. Dignon, Changes in the geographical distributions of global emissions of NOx and SOx from fossil-fuel combustion between 1966 and 1980, Atmos. Environment, 22, 441-449, 1988.

Houghton, / D. D., Handbook of applied meteorology, Wiley, N.Y., 1985.

Huebert, B. J., and C. H. Robert, The dry deposition of nitric acid to grass, J. Geophys. Res., 90, 2085-2090, 1985.

JPL, / NASA National Aeronautics and Space Administration, Chemical kinetics and photochemical data for use in stratospheric modeling. Evaluation number 9, JPL 90-1, Pasadena/CA., 1990.

Logan, J. A., Nitrogen oxides in the troposphere: Global and regional budgets,, J. Geophys. Res., 88, 10785-10807, 1983.

Logan, J. A., M. J. Prather, S. C. Wofsy, and M. B. McElroy, Tropospheric chemistry: A global perspective, J. Geophys. Res., 86, 7210-7254, 1981.

Marenco, A., and F. Said, Meridional aand vertical ozone distribution in the background troposphere (70°N-60°S; 0-12km altitude) from scientific aircraft measurements during the STRATOZ III experiment (June 1984), Atmos. Environment, 23, 201-214, 1989.

Murgatroyd, R. J., Estimations from geotrophic trajectories of horizontal diffusivity in the mid-latitude troposphere and lower stratosphere, Quart. J. Roy. Met. Soc., 95, 40-62, 1969.

Nueßer, H.-G., A. Schmitt, The global distribution of air traffic at high altitudes, related fuel consumption and trends, in Air traffic and the environment - background, tendencies and potential global atmospheric effects, pp 1-11, edited by U. Schumann, Springer Verlag, Berlin, 1990.

Penner, J. E., C. S. Atherton, J. Dignon, S. J. Ghan, J. J. Walton, and S. Hameed, Tropospheric nitrogen: a three-dimensional study of sources, distributions, and deposition, JGR, 96, 959-990, 1991.

Reichow, H.-P., Fuel consumption and emissions of air traffic, in Air traffic and the environment - background, tendencies and potential global atmospheric effects, pp 12-22, edited by U. Schumann, Springer Verlag, Berlin, 1990.

Roeth, E. P., Description of a one-dimensional model of atmospheric chemistry, in Juel - Bericht, vol. 2098 KFA Juelich, Juelich, 1986.

Rudolph, J., Two-Dimensional Distribution of Light Hydrocarbons: Results From the STRATOZ III Experiment, J. Geophys. Res., 93, 8367-8377, 1988.

Rudolph, J., B. Vierkorn-Rudolph, and F. X. Meixner, Large-scale distribution of peroxyacetylnitrate results from the STRATOZ III flights, J. Geophys. Res., 92, 6653-6661, 1987.

U.S. standard atmosphere, 1976 GPO, Washington, 1976.

Volz, A., D. H. Ehhalt, and R. G. Derwent, Seasonal and latitudinal variation of 14CO and the tropospheric concentration of OH radicals, J. Geophys. Res., 86, 5163-5171, 1981.

Wang, W. C., and N. D. Sze, Coupled effects of atmospheric N2O and O3 on the earth's climate, Nature, 286, 589-590, 1980.

Jül-2468
June 1991
ISSN 0366-0885